ESC European Society of Cardiology

European Heart Journal (2024) **00**, 1–17
https://doi.org/10.1093/eurheartj/ehae379

TRANSLATIONAL SCIENCE
Vascular biology and medicine

TRAP1 drives smooth muscle cell senescence and promotes atherosclerosis via HDAC3-primed histone H4 lysine 12 lactylation

Xuesong Li[1†], Minghong Chen[1†], Xiang Chen[1†], Xian He[1], Xinyu Li[1], Huiyuan Wei[1], Yongkang Tan[1], Jiao Min[1], Tayyiba Azam[2], Mengdie Xue[3], Yunjia Zhang[1], Mengdie Dong[1], Quanwen Yin[1], Longbin Zheng[1], Hong Jiang[1], Da Huo[3], Xin Wang[2], Shaoliang Chen[4]*, Yong Ji[5,6]*, and Hongshan Chen [1,7,8]*

[1]Key Laboratory of Cardiovascular and Cerebrovascular Medicine, School of Pharmacy, Nanjing Medical University, Nanjing 211166, China; [2]Faculty of Biology, Medicine and Health, University of Manchester, Manchester, UK; [3]Department of Medicinal Chemistry, Key Laboratory of Cardiovascular and Cerebrovascular Medicine, School of Pharmacy, Nanjing Medical University, Nanjing 211166, China; [4]Department of Cardiology, Nanjing First Hospital, Nanjing Medical University, Nanjing, China; [5]Key Laboratory of Cardiovascular and Cerebrovascular Medicine, Key Laboratory of Targeted Intervention of Cardiovascular Disease, Collaborative Innovation Center for Cardiovascular Disease Translational Medicine, State Key Laboratory of Reproductive Medicine, School of Pharmacy, the Affiliated Suzhou Hospital of Nanjing Medical University, Gusu School, Nanjing Medical University, Nanjing, Jiangsu, China; [6]National Key Laboratory of Frigid Zone Cardiovascular Diseases (NKLFZCD), Department of Pharmacology (State-Province Key Laboratories of Biomedicine-Pharmaceutics of China), College of Pharmacy, Key Laboratory of Cardiovascular Medicine Research and Key Laboratory of Myocardial Ischemia, Chinese Ministry of Education, NHC Key Laboratory of Cell Transplantation, the Central Laboratory of the First Affiliated Hospital, Harbin Medical University, Harbin, Heilongjiang, China; [7]Key Laboratory of Targeted Intervention of Cardiovascular Disease, Collaborative Innovation Center for Cardiovascular Disease Translational Medicine, Nanjing Medical University, Nanjing 211166, China; and [8]Department of Cardiovascular Surgery, The First Affiliated Hospital of Nanjing Medical University, Nanjing, Jiangsu 211166, China

Received 11 August 2023; revised 12 December 2023; accepted 3 June 2024

Abstract

Background and Aims Vascular smooth muscle cell (VSMC) senescence is crucial for the development of atherosclerosis, characterized by metabolic abnormalities. Tumour necrosis factor receptor-associated protein 1 (TRAP1), a metabolic regulator associated with ageing, might be implicated in atherosclerosis. As the role of TRAP1 in atherosclerosis remains elusive, this study aimed to examine the function of TRAP1 in VSMC senescence and atherosclerosis.

Methods TRAP1 expression was measured in the aortic tissues of patients and mice with atherosclerosis using western blot and RT–qPCR. Senescent VSMC models were established by oncogenic Ras, and cellular senescence was evaluated by measuring senescence-associated β-galactosidase expression and other senescence markers. Chromatin immunoprecipitation (ChIP) analysis was performed to explore the potential role of TRAP1 in atherosclerosis.

Results VSMC-specific TRAP1 deficiency mitigated VSMC senescence and atherosclerosis via metabolic reprogramming. Mechanistically, TRAP1 significantly increased aerobic glycolysis, leading to elevated lactate production. Accumulated lactate promoted histone H4 lysine 12 lactylation (H4K12la) by down-regulating the unique histone lysine delactylase HDAC3. H4K12la was enriched in the senescence-associated secretory phenotype (SASP) promoter, activating SASP transcription and exacerbating VSMC senescence. In VSMC-specific *Trap1* knockout $Apoe^{KO}$ mice ($Apoe^{KO}Trap1^{SMCKO}$), the plaque area, senescence markers, H4K12la, and SASP were reduced. Additionally, pharmacological inhibition and proteolysis-targeting chimera (PROTAC)-mediated TRAP1 degradation effectively attenuated atherosclerosis *in vivo*.

Conclusions This study reveals a novel mechanism by which mitonuclear communication orchestrates gene expression in VSMC senescence and atherosclerosis. TRAP1-mediated metabolic reprogramming increases lactate-dependent H4K12la via HDAC3, promoting SASP expression and offering a new therapeutic direction for VSMC senescence and atherosclerosis.

* Corresponding author. Tel: +86 25 8686 8467, Fax: +86 25 8686 8467, Email: hongshanchen@njmu.edu.cn, yongji@hrbmu.edu.cn, Chmengx@126.com
† The first three authors contributed equally to this work.

Structured Graphical Abstract

Key Question

The role of tumor necrosis factor receptor-associated protein 1 (TRAP1) in vascular smooth muscle cell (VSMC) senescence and atherosclerosis is unclear.

Key Finding

- Increased TRAP1 expression promoted VSMC senescence and atherosclerosis.
- TRAP1 drove histone H4 lysine 12 lactylation via metabolic reprogramming, inducing senescence-associated secretory phenotype and VSMC senescence.
- TRAP1 inhibition reduced atherosclerosis severity.

Take Home Message

These novel findings show that mitonuclear communication orchestrates gene expression associated with VSMC senescence and atherosclerosis. Inhibition of TRAP1-mediated metabolic reprogramming is a potential therapeutic target to reduce VSMC senescence and atherosclerosis.

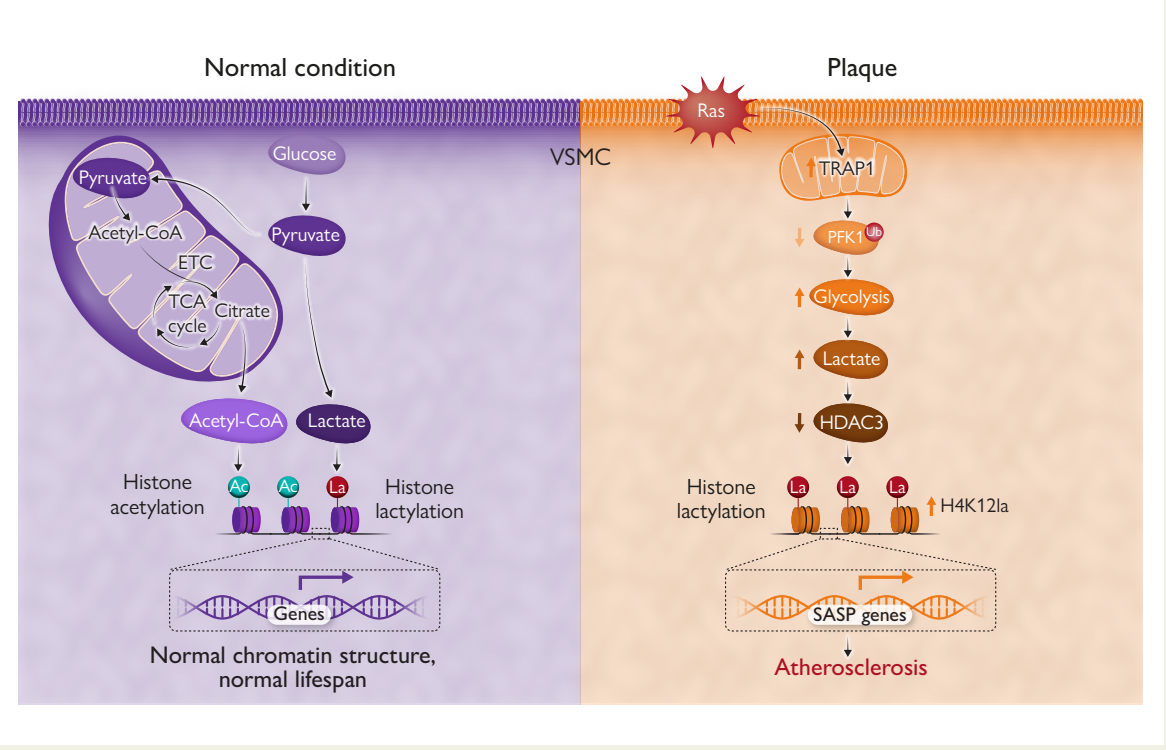

The proto-oncogene Ras induces aberrant TRAP1 expression in VSMCs, leading to metabolic reprogramming by increasing the levels of the glycolytic rate-limiting enzyme PFK1. Lactate accumulation increases H4K12la expression by blocking the unique histone delactylase, HDAC3. In this case, H4K12la is enriched at the SASP promoter region and promotes SASP transcription mediating VSMC senescence and promoting atherosclerosis. CoA, coenzyme A; ETC, electron transport chain; H4K12la, histone H4 lysine 12 lactylation; PFK1, phosphofructokinase 1; SASP, senescence-associated secretory phenotype; TCA, tricarboxylic acid; TRAP1, tumour necrosis factor receptor-associated protein 1; VSMC, vascular smooth muscle cell.

Keywords Senescence • Atherosclerosis • TRAP1 • Smooth muscle cells • Histone lactylation • HDAC3

Translational perspective

This study reveals that the link between epigenetic regulation and metabolism during senescence depends on TRAP1-activated histone lactylation mediated by the unique histone delactylase HDAC3. The discovery offers new insights into the potential delay in cellular senescence and the progression of atherosclerosis. Various experimental techniques, including gene manipulation, pharmacological inhibition, and PROTAC, have demonstrated that TRAP1 may serve as a promising target for the treatment of atherosclerosis.

Introduction

Atherosclerosis, a complex ageing-related disease, is a leading global cause of mortality.[1] Growing evidence suggests a pivotal role for vascular smooth muscle cell (VSMC) senescence in atherogenesis.[2] VSMC senescence contributes to diminished VSMC content and adversely affects post-rupture plaque repair, thereby promoting plaque vulnerability.[3] Recently, a promising category of drugs known as 'senolytics', specifically designed to selectively target and eliminate senescent cells, has emerged with potential therapeutic applications for atherosclerosis.[3] However, the considerable side effects of these senolytics limit their applicability and suitability for patient use. Consequently, elucidating the novel mechanisms of VSMC senescence and identifying new therapeutic targets is imperative for advancing the treatment of atherosclerosis.

Cellular senescence is characterized by an irreversible growth arrest triggered by cellular stress.[4] Various factors contribute to this phenomenon, including mitochondrial dysfunction, aberrant oncogene activation, and epigenetic alterations.[5] Senescent cells release a diverse array of bioactive factors known as senescence-associated secretory phenotype (SASP), disrupting the tissue microenvironment and contributing to senescence-related inflammation.[6] Studies of the mechanisms underlying VSMC senescence in atherosclerosis have predominantly focused on telomere length and oxidative stress.[7] However, a noticeable research gap exists concerning the epigenetic regulation of SASP in VSMC senescence and atherosclerosis.

Epigenetic alterations and metabolic dysfunctions are important hallmarks of senescence. Numerous studies have highlighted the close association between cellular metabolism and epigenetic modifications in senescent cells.[8] Acetyl-coenzyme A (acetyl-CoA), a metabolic focal point, plays a pivotal role in histone acetylation and influences gene expression in several degenerative diseases.[9] The endogenous intermediate metabolite, α-ketoglutarate, possesses the ability to drive and modulate nuclear gene expression via histone methylation profiles.[8] Therefore, investigating the intricate cross-talk between metabolic and epigenetic regulation in senescence is a compelling avenue for investigation.

Senescent VSMCs undergo the metabolic transition from mitochondrial oxidative phosphorylation to aerobic glycolysis, which is primarily attributed to mitochondrial dysfunction. Consequently, this transition leads to the production of large amounts of the glycolytic metabolite lactate.[10] Lactate, integral to numerous physiological processes, serves as a key regulator of signalling transduction and energy metabolism.[11] However, excessively elevated lactate levels can exacerbate various diseases, including heart failure, pulmonary hypertension, and cancer.[12–14] Moreover, increased lactate levels have been proposed as a marker of ageing.[15]

Tumour necrosis factor receptor-associated protein 1 (TRAP1), a prominent mitochondrial member of the heat shock protein 90 (HSP90) family, plays a crucial role in modulating metabolism and organelle homeostasis in health and disease.[16,17] TRAP1 induces lactate accumulation via aerobic glycolysis, contributing to metabolic reprogramming that supports tumour growth.[18] Moreover, TRAP1 plays a substantial role in ageing-related diseases, such as macular degeneration and Parkinson's disease.[19,20]

Accumulating evidence suggests that alterations in histone modification are predisposing factors for senescence.[21] Enrichment of histone H3 lysine 4 trimethylation (H3K4me3) in promoters can activate senescence-related genes, leading to senescence.[22] Recently, a novel epigenetic modification of lactate-derived histone lactylation was shown to directly regulate gene transcription.[23] Notably, in Alzheimer's disease, attenuating microglial glycolysis and reducing histone lactylation ameliorate Aβ burden and cognitive impairment.[24] Therefore, targeting histone modifications is a promising therapeutic strategy for addressing senescence.

Although TRAP1 expression is elevated in ruptured plaques in atherosclerosis, the specific role of TRAP1 in atherosclerosis remains unexplored.[25] This present study aimed to fill this knowledge gap by comprehensively investigating the role of TRAP1 in VSMC senescence and atherosclerosis. To assess the impact of TRAP1 on VSMC senescence and atherosclerosis, we employed Ras-induced senescent VSMCs as the cellular model and generated SMC-specific *Trap1*-knockout mice on the *Apoe*^{KO} background (*Apoe*^{KO}*Trap1*^{SMCKO}). Additionally, pharmacological inhibition and proteolysis-targeting chimera (PROTAC) were utilized to degrade TRAP1 for functional analysis and validation. These approaches aim to comprehensively evaluate the role of TRAP1 during VSMC senescence and atherosclerosis.

Methods

Detailed methods are provided in the Supplementary material.

Results

TRAP1 regulates VSMC senescence

Mitochondrial dysfunction is important in the initiation of cellular senescence.[26] To identify novel associations between mitochondria and senescence, we integrated the senescence database (https://ngdc.cncb.ac.cn/aging/index) and MitoMiner database (https://www.broadinstitute.org/mitocarta/mitocarta30-inventory-mammalian-mitochondrial-proteins-and-pathways). As illustrated in the Sankey diagram in Supplementary data online, *Figure S1A*, the red arcs represent non-senescent-associated mitochondrial genes, following the flow from right to left. Conversely, blue arcs depict senescence genes independent of the mitochondria, flowing from left to right. Notably, 35 mitochondrial genes (purple) were associated with senescence.[27] Next, we profiled the expression of these genes in proto-oncogene Ras-induced human VSMCs (hVSMCs) using reverse transcription–quantitative polymerase chain reaction (RT–qPCR). Notably, TRAP1 was identified as a novel senescence-associated gene significantly up-regulated in Ras-induced hVSMCs based on the volcano plot (*Figure 1A*). Therefore, we hypothesized that TRAP1 participates in the regulation of cellular senescence. To clarify whether the increased TRAP1 in atherosclerotic plaques is accompanied by senescence, we measured the expression of TRAP1 and typical senescence markers (P53, P21, and P16) in the aortic tissues of atherosclerotic patients and high-fat diet (HFD)-fed *Apoe*^{KO} mice.[28] The results revealed a notable increase in TRAP1 expression and senescence markers (P53, P21, and P16) in the aortic tissues of atherosclerotic patients (*Figure 1B*; Supplementary data online, *Figure S1B*) and HFD-fed *Apoe*^{KO} mice (*Figure 1C*; Supplementary data online, *Figure S1C and D*). In addition, TRAP1 and α-smooth muscle actin (α-SMA) exhibited strong co-localization in plaques from HFD-fed *Apoe*^{KO} mice compared with those from control mice, whereas no significant TRAP1 co-localization was observed with CD31 or CD68 (see Supplementary data online, *Figure S1E*). Similar patterns were observed in Ras-induced hVSMCs, human peripheral blood monocytes, and human aortic endothelial cells (*Figure 1D and E*; Supplementary data online, *Figure S1F–I*). Together, these findings indicate that TRAP1 expression is up-regulated in atherosclerosis, primarily in VSMCs. Furthermore, we demonstrated that TRAP1 deficiency prevented the elevation of senescence markers in Ras-induced hVSMCs

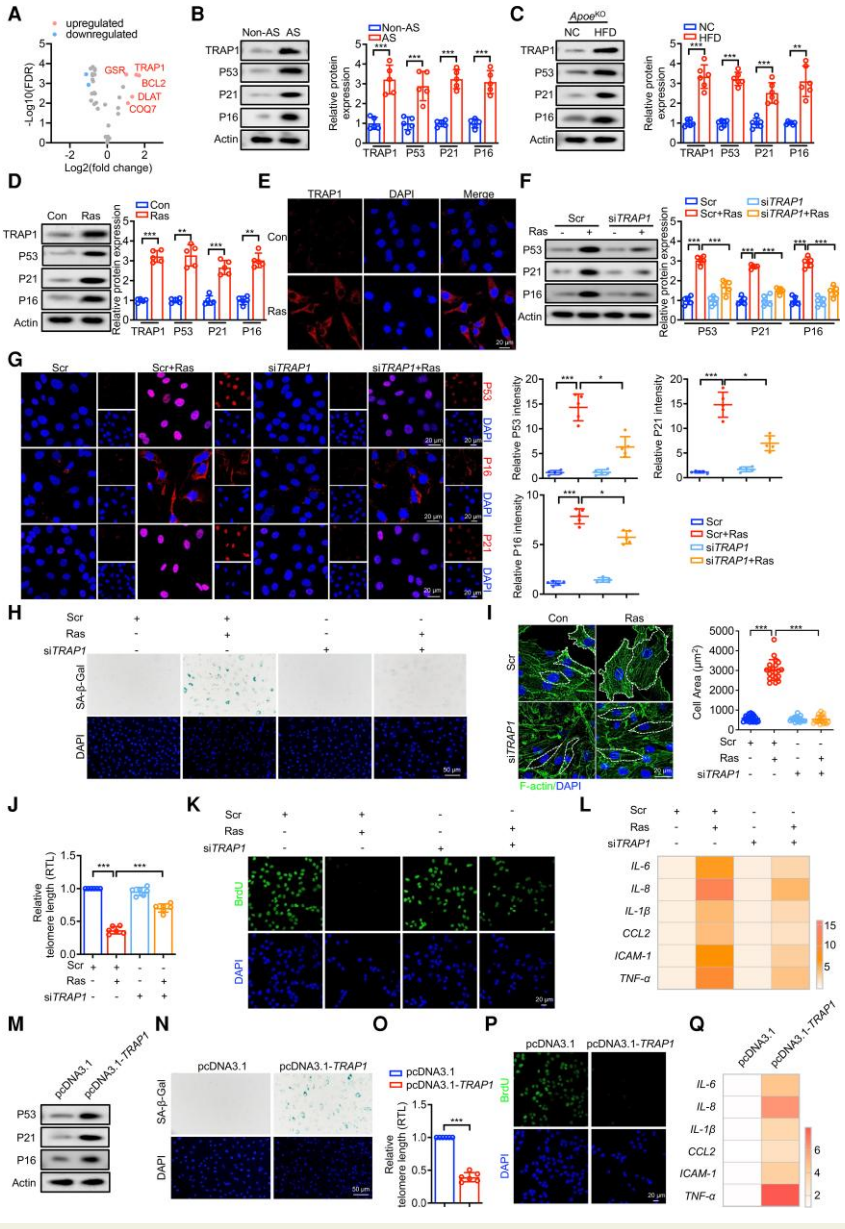

Figure 1 TRAP1 regulates VSMC senescence. (*A*) The volcano graph shows the distribution of differentially expressed genes. Red dots represent up-regulated genes, and blue dots represent down-regulated genes. (*B*) Western blot analysis of TRAP1 and senescence markers in the aortic tissues of the non-atherosclerotic (Non-AS) and atherosclerotic (AS) groups ($n = 5$ independent biological replicates). (*C*) Western blot analysis of TRAP1 and senescence markers in the aortic tissues from NC- and HFD-fed *Apoe*^{KO} mice ($n = 6$ independent biological replicates). (*D*) Western blot analysis of TRAP1 and senescence markers in Ras-induced hVSMCs ($n = 5$ independent biological replicates). (*E*) Representative immunofluorescence staining images of TRAP1 (red) and 4',6-diamidino-2-phenylindole (DAPI; blue) expression in Ras-induced hVSMCs (scale bar = 20 μm, $n = 5$ independent biological replicates). (*F*) Western blot analysis of senescence markers in Ras-induced hVSMCs transfected with si*TRAP1* ($n = 5$ independent biological replicates). (*G*) Representative immunofluorescence staining images of senescence markers (red) and DAPI (blue) in Ras-induced hVSMCs transfected with si*TRAP1* (scale bar = 20 μm, $n = 5$ independent biological replicates). (*H*) SA-β-Gal staining of Ras-induced hVSMCs transfected with si*TRAP1* (scale bar = 50 μm, $n = 5$ independent biological replicates). (*I*) Super-resolution fluorescence imaging of F-actin in Ras-induced hVSMCs transfected with si*TRAP1* (scale bar = 20 μm, $n = 5$ independent biological replicates). (*J*) Relative telomere length in Ras-induced hVSMCs transfected with si*TRAP1* ($n = 6$ independent biological replicates). (*K*) Proliferation measured using the bromodeoxyuridine (BrdU) assay in Ras-induced hVSMCs transfected with si*TRAP1* (scale bar = 20 μm, $n = 5$ independent biological replicates). (*L*) Heatmap showing the relative expression of SASP in Ras-induced hVSMCs transfected with si*TRAP1* ($n = 6$ independent biological replicates). (*M*) Western blot analysis of senescence markers in hVSMCs overexpressing *TRAP1* ($n = 5$ independent biological replicates). (*N*) SA-β-Gal staining of hVSMCs overexpressing *TRAP1* (scale bar = 50μm, $n = 5$ independent biological replicates). (*O*) Relative telomere length in hVSMCs overexpressing *TRAP1* ($n = 6$ independent biological replicates). (*P*) Proliferation measured using the BrdU assay in hVSMCs overexpressing *TRAP1* (scale bar = 20 μm, $n = 5$ independent biological replicates). (*Q*) Heatmap showing the relative expression of SASP in hVSMCs overexpressing *TRAP1* ($n = 6$ independent biological replicates). $^*P < .05$, $^{**}P < .01$, $^{***}P < .001$. Data are presented as the mean ± SD. Unpaired *t*-test was used for comparison in (B–D). Welch's correction was used for comparison in (C) and (O). One-way analysis of variance (ANOVA) was performed for comparison (F and G, and I and J)

(*Figure 1F* and *G*; Supplementary data online, *Figure S1J*). The senescence of VSMCs is characterized by a phenotypic switch.[29] Ras induced a significant decrease in the mRNA and protein expression of contractile phenotype-related genes (*Myocardin*, *α-SMA*, *CNN1*, *MYH11*, and *Tagln*) in VSMCs, along with an increased mRNA and protein expression of synthetic phenotype-related genes (*OPN* and *MMP2*), which were prevented by TRAP1 deletion (see Supplementary data online, *Figure S1K* and *L*). Similarly, the number of senescence-associated β-galactosidase-(SA-β-Gal) positive cells and the area of enlarged VSMCs were significantly decreased in Ras-induced hVSMCs with TRAP1 deficiency (*Figure 1H* and *I*; Supplementary data online, *Figure S1M*), accompanied by restoration of telomere length and cell proliferation capacity (*Figure 1J* and *K*). Moreover, TRAP1 silencing substantially reduced the up-regulation of SASP in Ras-induced senescent hVSMCs (*Figure 1L*; Supplementary data online, *Figure S1N*). Furthermore, we generated hVSMCs with stable TRAP1 overexpression (Supplementary data online, *Figure S1O*) and found that TRAP1 overexpression significantly promoted VSMC senescence (*Figure 1M–Q*; Supplementary data online, *Figure S1P–R*). Cumulatively, our data revealed that TRAP1, a senescence-associated mitochondrial gene, actively promotes senescence in VSMCs.

TRAP1 is a key regulator of energy reprogramming in senescent VSMCs

Increasing evidence confirms that mitochondrial dysfunction drives metabolic reprogramming in senescent cells.[30] Given its pivotal role as a regulator of mitochondrial bioenergetics,[31] TRAP1 is speculated to be involved in energy conversion in senescent VSMCs. As TRAP1 is predominantly localized in the mitochondria,[17] our initial investigation focused on whether TRAP1 affects mitochondrial function in Ras-induced hVSMCs. Consistently, TRAP1 was primarily localized to the mitochondria in Ras-induced hVSMCs, as observed via total internal reflection fluorescence microscopy (see Supplementary data online, *Figure S2A*). TRAP1 deficiency ameliorated the mitochondrial damage, the decreased oxygen consumption rate (OCR), and the increased extracellular acidification rate (ECAR) in Ras-induced hVSMCs (*Figure 2A–C*). Furthermore, TRAP1 deficiency up-regulated the levels of acetyl-CoA and citrate, which are essential for ATP production via mitochondrial oxidative phosphorylation (*Figure 2D* and *E*). These changes suggested that TRAP1 deficiency mitigated the shift towards glycolysis in energy metabolism in Ras-induced VSMCs. Furthermore, we examined the expression and activity of the corresponding enzymes involved in energy metabolism. Hexokinase 2 (HK2), pyruvate kinase M2 (PKM2), and phosphofructokinase 1 (PFK1) are three crucial glycolytic rate-limiting enzymes[32] (see Supplementary data online, *Figure S2B*). In addition to assessing glycolytic rate-limiting enzyme expression (HK2, PKM2, and PFK1) in Ras-induced VSMCs treated with small interfering *TRAP1* (si*TRAP1*), we simultaneously screened for the expression and activity of enzymes involved in oxidative phosphorylation [mitochondrial tricarboxylic acid (TCA) cycle enzymes and electron transport chain complexes] (*Figure 2F* and *G*; Supplementary data online, *Figure S2C–G*). The expression of the glycolytic rate-limiting enzyme PFK1 was significantly up-regulated in Ras-induced VSMCs, recovered via si*TRAP1*. This result was also confirmed using the TRAP1 pharmacological inhibitor gamitrinib-triphenylphosphonium (G-TPP) (*Figure 2H* and *I*; Supplementary data online, *Figure S2H*). In contrast, the expression of enzymes in the TCA cycle and electron transport chain, and the activity of TCA cycle enzymes were unchanged in Ras-induced VSMCs with or without TRAP1 deficiency (see Supplementary data online, *Figure S2C–F*). The enzymatic activity of the electron transport chain complex IV increased in Ras-induced VSMCs after TRAP1 deficiency (see Supplementary data online, *Figure S2G*). The PFK1 metabolite fructose-1,6-bisphosphate (F-1,6-BP) strongly inhibits the activity of complex IV.[33] Thus, we assumed that the effect of TRAP1 on complex IV was dependent on PFK1. Subsequently, we knocked down PFK1 and detected the activity of electron respiratory chain complex IV in TRAP1-overexpressing VSMCs. The results showed that compared with TRAP1-overexpressing VSMCs, the activity of complex IV was up-regulated in TRAP1-overexpressing VSMCs treated with si*PFK1* (see Supplementary data online, *Figure S2I*). Therefore, these results confirmed that TRAP1 up-regulation in senescent VSMCs reduced OCR due to inhibiting complex IV activity via increased PFK1 expression. Based on these findings, we next focused on the PFK1-mediated glycolysis pathway. Furthermore, the BioGRID database (https://thebiogrid.org/) revealed potential interactions between TRAP1 and PFK1[18,34] (see Supplementary data online, *Figure S2J*). These results implied that TRAP1 mediates glycolysis by interacting with PFK1. As expected, the interaction between TRAP1 and PFK1 was strengthened in Ras-induced hVSMCs (*Figure 2J*). Additionally, we observed that TRAP1 promoted PFK1 expression by decreasing its ubiquitination level, consistent with earlier results[18] (see Supplementary data online, *Figure S2K–N*). Meanwhile, the PFK1 inhibitor citrate improved energy metabolism in TRAP1-overexpressing hVSMCs (*Figure 2K* and *L*). Collectively, these data indicated that TRAP1 up-regulates glycolysis by regulating PFK1 expression in senescent hVSMCs.

TRAP1-mediated lactate accumulation promotes VSMC senescence

Given the notable up-regulation of glycolysis in senescent hVSMCs, it was important to explore the involvement of lactate, a key metabolite of glycolysis, in hVSMC senescence. As shown in *Figure 3A*, elevated lactate production was decreased in senescent hVSMCs treated with si*TRAP1*. Furthermore, exogenous lactate supplementation reversed the decreased hVSMC senescence caused by treatment with si*TRAP1*, including expression of senescence markers, the cell proliferative capacity, the number of SA-β-Gal-positive cells, and SASP expression (*Figure 3B–E*; Supplementary data online, *Figure S3A*). These results demonstrated that TRAP1-induced senescence in VSMCs is caused by lactate accumulation. To further validate this finding, we decreased the lactate production using the glycolysis inhibitor 2-deoxy-D-glucose (2-DG), the lactate dehydrogenase inhibitor oxamate, and siRNA-targeting lactate dehydrogenase (si*LDHA*) (see Supplementary data online, *Figure S3B*). In agreement with our hypotheses, a reduction in lactate levels significantly attenuated VSMC senescence (*Figure 3F–K*). Collectively, these findings support the hypothesis that TRAP1 induced cellular senescence by increasing lactate accumulation.

TRAP1-mediated-H4 lysine 12 lactylation (H4K12la) promotes SASP activation in senescent VSMCs

To investigate the mechanism by which increased lactate levels promote SASP, we first assessed the levels of protein lactylation in Ras-induced hVSMCs. As shown in *Figure 4A*, global protein lactylation levels markedly increased, and this effect was reversed by si*TRAP1*. Notably, a distinct band around histone locations was observed, which prompted us to focus on alterations in histone lactylation. Subsequently, we examined several previously confirmed sites of

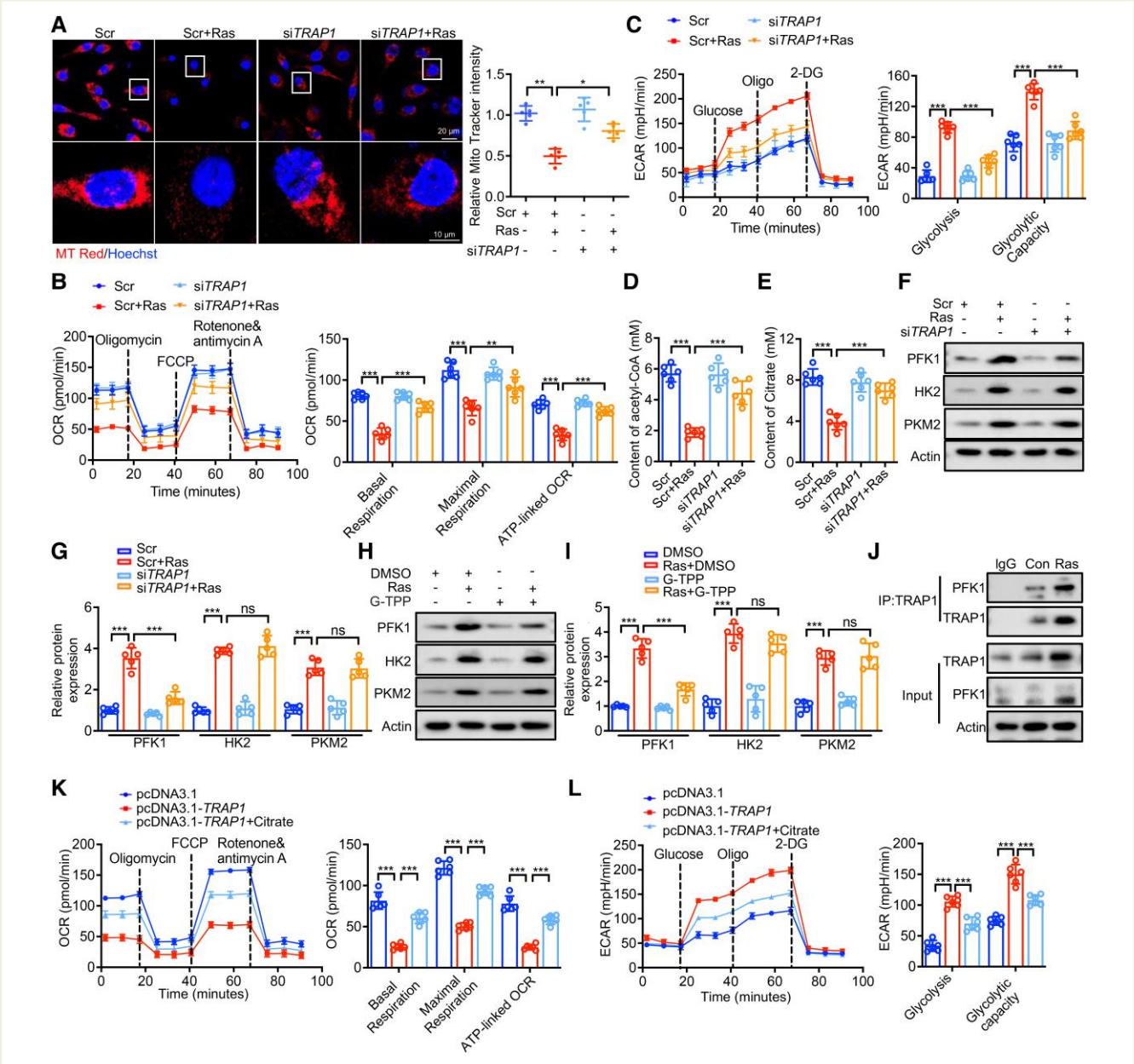

Figure 2 TRAP1 is a key regulator of energy reprogramming in senescent VSMCs. (*A*) Assessment of mitochondrial quality based on Mito Tracker Red staining of Ras-induced hVSMCs transfected with si*TRAP1* (scale bar = 20 μm, $n = 5$ independent biological replicates). (*B*) OCR of Ras-induced hVSMCs transfected with si*TRAP1* was monitored in real-time using the seahorse system. OCR was used as a marker of mitochondrial respiration (left panel), and the basal respiration, maximal respiration, and ATP-linked OCR were assessed (right panel, $n = 6$ independent biological replicates). (*C*) ECAR of Ras-induced hVSMCs transfected with si*TRAP1* was monitored in real-time using the seahorse system. ECAR was used primarily to measure glycolysis (left panel) and assess cellular glycolysis and glycolytic capacity (right panel, $n = 6$ independent biological replicates). (*D*) Detection of acetyl-CoA levels in Ras-induced hVSMCs following TRAP1 deficiency ($n = 6$ independent biological replicates). (*E*) Detection of citrate levels in Ras-induced hVSMCs following TRAP1 deficiency ($n = 6$ independent biological replicates). (*F*) Western blot analysis of PFK1, HK2, and PKM2 protein levels in Ras-induced hVSMCs following TRAP1 deficiency ($n = 5$ independent biological replicates). (*G*) Quantification of protein levels of the blots shown in (F) ($n = 5$ independent biological replicates). (*H*) Western blot analysis of PFK1, HK2, and PKM2 protein levels in Ras-induced hVSMCs treated with 1 μM G-TPP for 4 h ($n = 5$ independent biological replicates). (*I*) Quantification of protein levels of the blots shown in (H) ($n = 5$ independent biological replicates). (*J*) Co-immunoprecipitation analysis of PFK1–TRAP1 binding in Ras-induced hVSMCs ($n = 5$ independent biological replicates). (*K*) Using the seahorse system, the OCR of TRAP1-overexpressing hVSMCs was monitored in real-time following citrate (1 mM) treatment for 6 h (left panel), assessing basal respiration, maximal respiration, and ATP-linked OCR (right panel, $n = 6$ independent biological replicates). (*L*) ECAR of TRAP1-overexpressing hVSMCs was monitored in real-time using seahorse technology following citrate (1 mM) treatment for 6 h (left panel), assessing cellular glycolysis and glycolytic capacity (right panel, $n = 6$ independent biological replicates). $^*P < .05$, $^{**}P < .01$, $^{***}P < .001$. Data are presented as the mean ± SD. One-way ANOVA was performed in (A–E, G, I, K, and L)

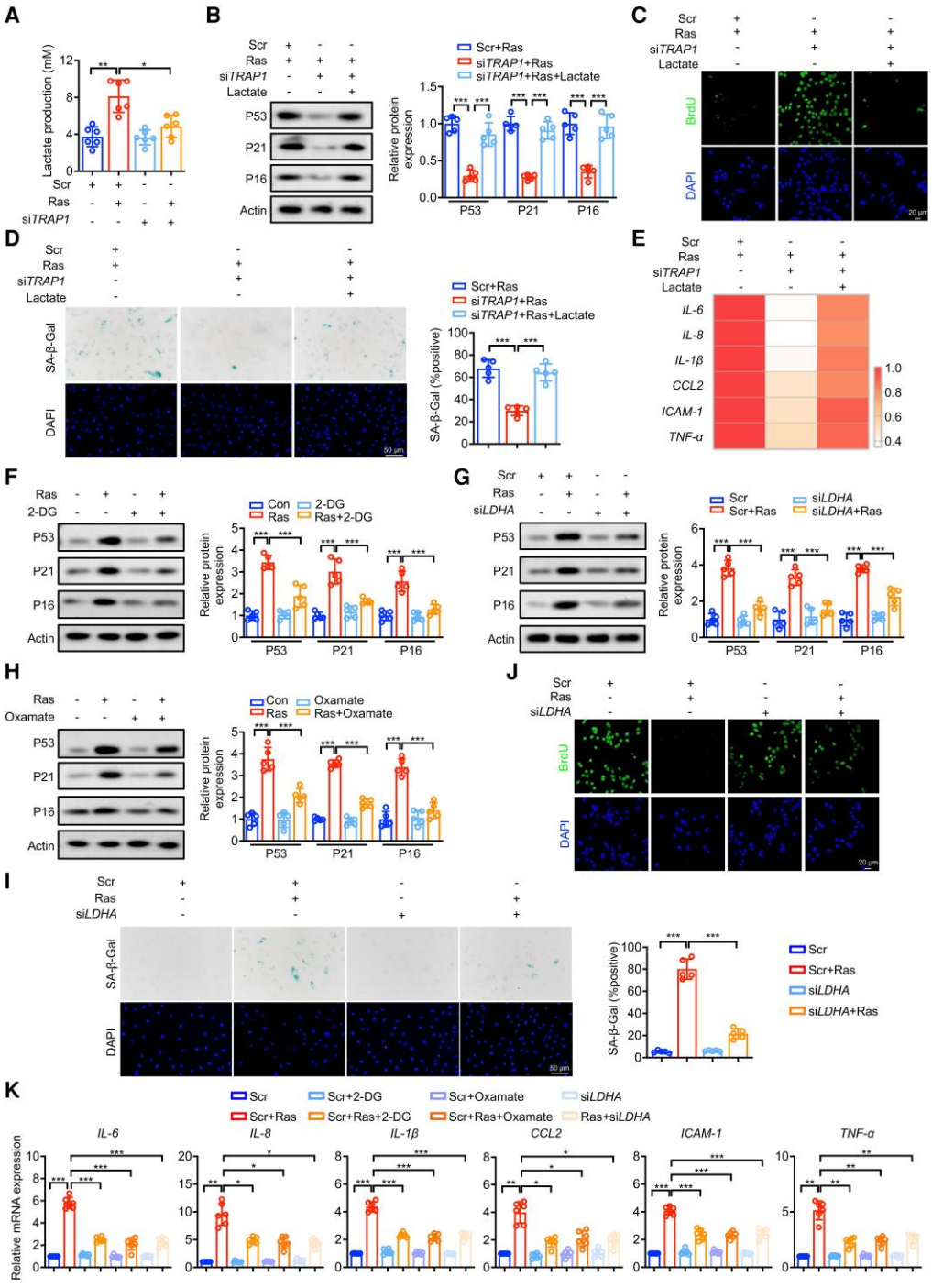

Figure 3 TRAP1-mediated lactate accumulation promotes VSMC senescence. (*A*) Detection of lactate levels in Ras-induced hVSMCs with TRAP1 deficiency ($n = 6$ independent biological replicates). (*B*) Western blot analysis of senescence markers levels in Ras-induced hVSMCs treated with si*TRAP1*, followed by treatment with or without exogenous lactate (5 mM) for 24 h ($n = 5$ independent biological replicates). (*C*) Proliferation was measured using BrdU assay in Ras-induced hVSMCs treated with si*TRAP1*, followed by treatment with or without exogenous lactate (scale bar = 20 μm, $n = 5$ independent biological replicates). (*D*) Representative SA-β-Gal staining images in Ras-induced hVSMCs treated with si*TRAP1*, followed by treatment with or without exogenous lactate (scale bar = 50 μm, $n = 5$ independent biological replicates). (*E*) RT–qPCR analysis of SASP expression in Ras-induced hVSMCs treated with si*TRAP1*, followed by treatment with or without exogenous lactate, presented as a heatmap ($n = 6$ independent biological replicates). (*F–H*) Senescence markers were detected in Ras-induced hVSMCs following 2-DG (*F*), si*LDHA* (*G*), and oxamate (*H*) treatment via western blot analysis ($n = 5$ independent biological replicates). (*I*) Representative SA-β-Gal staining images in Ras-induced hVSMCs treated with si*LDHA* (scale bar = 50 μm, $n = 5$ independent biological replicates). (*J*) Proliferation measured using the BrdU assay in Ras-induced hVSMCs treated with si*LDHA* (scale bar = 20 μm, $n = 5$ independent biological replicates). (*K*) RT–qPCR was used to detect SASP expression in Ras-induced senescent hVSMCs treated with 2-DG, oxamate, and si*LDHA* ($n = 6$ independent biological replicates). $^{*}P < .05$, $^{**}P < .01$, $^{***}P < .001$. Data are presented as the mean ± SD. One-way ANOVA was performed in (A, B, D, F–I, and K)

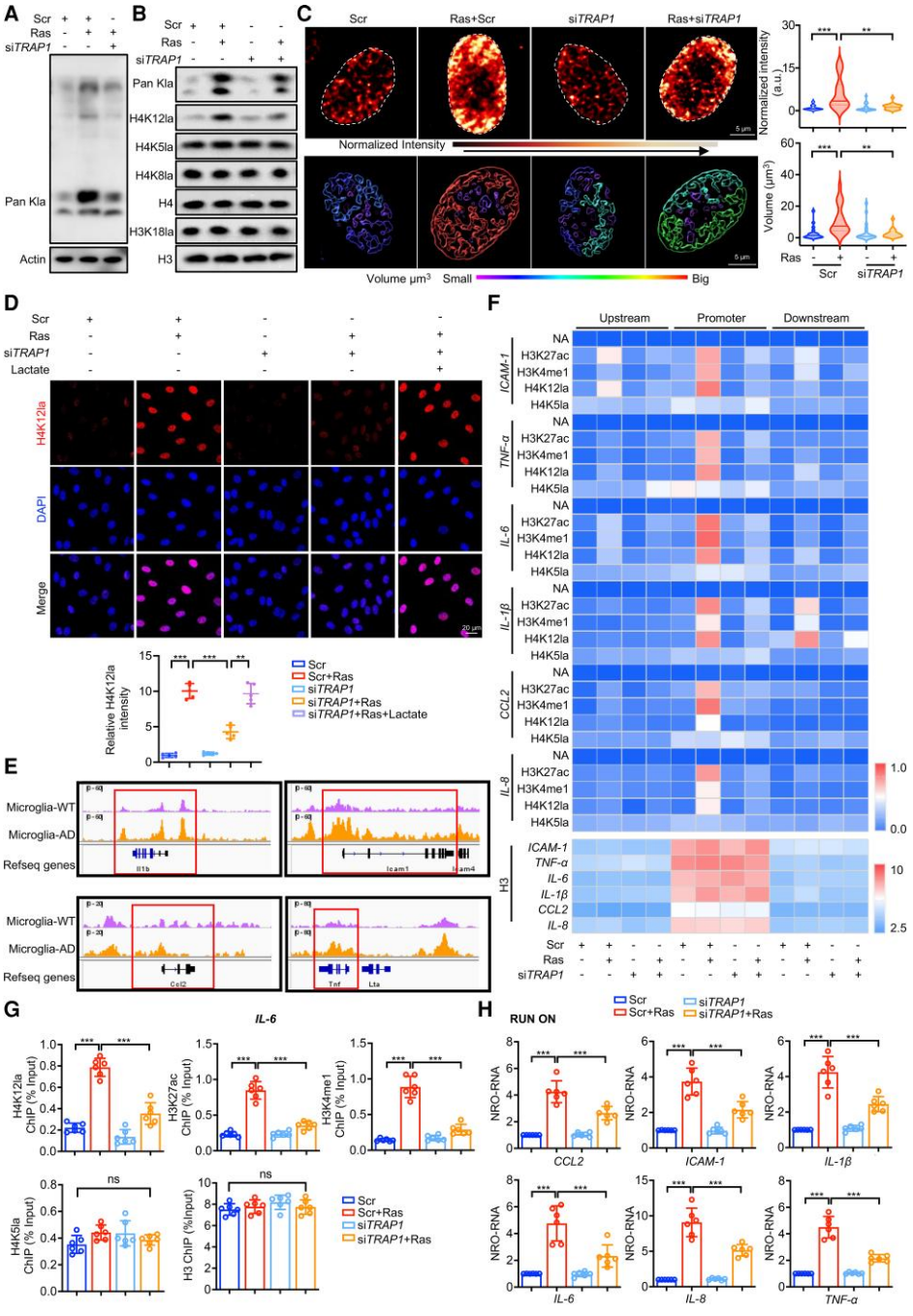

Figure 4 TRAP1-mediated H4K12la promotes SASP activation in senescent VSMCs. (*A*) Western blot analysis of Pan Kla protein levels in Ras-induced hVSMCs following TRAP1 deficiency ($n = 5$ independent biological replicates). (*B*) Western blot analysis of Pan Kla, H4K12la, H4K5la, H4K8la, and H3K18la levels in Ras-induced hVSMCs following TRAP1 deficiency ($n = 5$ independent biological replicates). (*C*) Expression levels of H4K12la in the nucleus of Ras-induced hVSMCs following TRAP1 deficiency, assessed using super-resolution fluorescence imaging (upper). Volume information of H4K12la hotspots identified in the nucleus of Ras-induced hVSMCs following TRAP1 deficiency (bottom) (scale bar = 5 μm, $n = 5$ independent biological replicates). (*D*) Representative images of H4K12la co-stained with DAPI in Ras-induced hVSMCs treated with si*TRAP1* or supplemented with exogenous lactate (5 mM) for 24 h (scale bar = 20 μm, $n = 5$ independent biological replicates). (*E*) Genome browser tracks of the ChIP-seq signals from GSE188765 at representative SASP loci. (*F*) The heatmap displayed the enrichment of H4K5la, H4K12la, H3K27ac, and H3K4me1 around the promoter region of SASP, ranging from −1 kb to +1 kb. The degree of binding of H3 to SASP was used as the positive control ($n = 6$ independent biological replicates). (*G*) Enrichment of H3K4me1, H4K12la, H3K27ac, and H4K5la at the interleukin-6 (IL-6) promoter analysed via ChIP-qPCR from the results of the heatmap in (F). Data are presented in the form of a column chart ($n = 6$ independent biological replicates). (*H*) Global nascent transcripts of SASP were measured using nuclear run-on experiments coupled with RT–qPCR in isolated nuclei from Ras-induced hVSMCs following si*TRAP1* treatment ($n = 6$ independent biological replicates). *$P < .05$, **$P < .01$, ***$P < .001$. Data are presented as the mean ± SD. One-way ANOVA was performed in (C, D, G, and H)

histone lactylation and found that only the H4K12la level was markedly elevated upon Ras stimulation, which was prevented by si*TRAP1* (*Figure 4B*; Supplementary data online, *Figure S4A*). This finding was further supported by super-resolution fluorescence imaging, as shown in *Figure 4C* (upper). However, the expression of other common H4 lactylation sites, including H4K5la and H4K8la, did not change.[23,24,35] Ras-induced condensation of H4K12la in VSMCs led to their enrichment in the nuclear envelope, which was prevented by si*TRAP1* (*Figure 4C*, bottom). Exogenous lactate supplementation restored the down-regulated H4K12la level in Ras-induced hVSMCs treated with si*TRAP1* (*Figure 4D*). To further confirm the contribution of H4K12la to SASP transcription, publicly available chromatin immunoprecipitation sequencing (ChIP-seq) data from Alzheimer's disease, a well-recognized ageing disease, were analysed.[24] The results demonstrated that the enrichment of H4K12la at the promoter of SASP was increased (*Figure 4E*). H3K27ac and H3K4me1 are classical epigenetic markers of activated genomic features, enhancing the transcription rate.[36] ChIP-qPCR analysis confirmed that Ras caused the enrichment of H4K12la at the SASP promoter in hVSMCs, along with two representative chromosome accessibility markers, H3K27ac and H3K4me1, and this was significantly suppressed by si*TRAP1* (*Figure 4F and G*; Supplementary data online, *Table S1*). To precisely monitor nascent mRNA transcription, we used a run-on transcription assay to detect gene transcription in real-time (see Supplementary data online, *Figure S4B*). We found that the bromouridine-triphosphate (Br-UTP)-labelled nascent transcripts of SASP were boosted after Ras treatment, which was prevented by si*TRAP1* (*Figure 4H*). Collectively, we identified a histone microenvironment labelled with H4K12la that promotes SASP transcription in Ras-induced hVSMCs.

Up-regulation of H4K12la by blocking HDAC3 promotes VSMC senescence

p300 is a potential lactylation writer protein, and HDAC1–3 are important regulators of delactylase activity.[37] However, the regulatory enzymes mediating histone lactylation in senescent hVSMCs remain unclear. We assessed the catalytic functions of representative p300 and HDAC1–3, and observed a significant decrease in HDAC3 protein expression in Ras-induced hVSMCs (*Figure 5A*; Supplementary data online, *Figure S5A*), thus identifying the involvement of HDAC3 in VSMC senescence. Previous studies have demonstrated that lactate could down-regulate HDAC3 protein expression.[38] Similarly, our results revealed that TRAP1 down-regulates HDAC3 protein expression via lactate in senescent hVSMCs (*Figure 5B–D*; Supplementary data online, *Figure S5B–D*). Western blot and immunofluorescence staining revealed a substantial reduction in H4K12la in HDAC3-overexpressing senescent hVSMCs (*Figure 5E–G*; Supplementary data online, *Figure S5E–H*). Furthermore, overexpression of HDAC3 significantly diminished the expression of senescence markers and SASP, while concurrently restoring cell proliferation (*Figure 5H–J*; Supplementary data online, *Figure S5I*). To further substantiate the impact of HDAC3 on SASP expression, a run-on transcription technique was employed, which revealed a notable reduction in Br-UTP-labelled nascent SASP transcripts in HDAC3-overexpressing senescent hVSMCs (*Figure 5K*). Furthermore, we used the HDAC agonist, ITSA-1, to confirm the role of HDAC3 in VSMC senescence mediated by H4K12la. ITSA-1 had the same effect as HDAC3 overexpression. HDAC3 activation effectively prevented the increase in H4K12la and senescence in Ras-induced VSMCs (*Figure 5G–K*). In comparison with Ras stimulation, ChIP-qPCR studies indicated that HDAC3 overexpression markedly reduced H4K12la enrichment, and diminished H3K27ac and H3K4me1 levels at the SASP promoter (*Figure 5L*; Supplementary data online, *Figure S5J*). These results suggested that HDAC3 overexpression decreased SASP transcription by down-regulating H4K12la in Ras-induced VSMCs. Re-ChIP analysis further revealed the decreased binding of HDAC3 and H4K12la to the SASP promoter (*Figure 5M*). Collectively, these results support the hypothesis that lactate increases H4K12la levels by suppressing HDAC3 expression, thereby promoting VSMC senescence.

SMC-specific *Trap1* knockout ameliorates atherosclerosis

To explore the role of TRAP1 in VSMCs *in vivo*, we generated SMC-specific *Trap1*-knockout mice with $Apoe^{KO}$ ($Apoe^{KO}Trap1^{SMCKO}$) and fed them with either normal chow (NC) or HFD for 16 weeks. Analysis of body weight and serum lipid levels of $Apoe^{KO}Trap1^{WT}$ mice showed no discernible difference from those of $Apoe^{KO}Trap1^{SMCKO}$ mice (see Supplementary data online, *Table S2*). The SMC-specific *Trap1* knockout efficiency was further confirmed via western blot and RT–qPCR (see Supplementary data online, *Figure S6A and B*). Oil Red O staining of the aortas showed that compared with HFD-fed $Apoe^{KO}Trap1^{WT}$ mice, the plaque area in the whole aorta was significantly reduced in HFD-fed $Apoe^{KO}Trap1^{SMCKO}$ mice (*Figure 6A*). Consistently, immunohistochemistry staining of the aortic root revealed decreased lipid accumulation, plaque area, and necrotic core size, along with increased collagen content in $Apoe^{KO}Trap1^{SMCKO}$ mice compared with those in $Apoe^{KO}Trap1^{WT}$ mice (*Figure 6B–D*). These data indicated that SMC-specific *Trap1* knockout effectively decreases plaque area and increases plaque stability. Additionally, immunofluorescence staining demonstrated a decrease in senescent SMCs in $Apoe^{KO}Trap1^{SMCKO}$ mice, as evidenced by decreased P21 (a senescence marker) expression and co-localization of P21 and α-SMA (a VSMC marker) (*Figure 6E*). H4K12la expression in SMCs was significantly lower in the aorta of $Apoe^{KO}Trap1^{SMCKO}$ mice than in $Apoe^{KO}Trap1^{WT}$ mice (*Figure 6F*). Furthermore, we isolated mouse aortic vascular smooth muscle cells (MOVAS) from HFD-fed $Apoe^{KO}Trap1^{SMCKO}$ and $Apoe^{KO}Trap1^{WT}$ mice. As depicted in *Figure 6G*, the expression levels of senescence markers and H4K12la increased in HFD-fed $Apoe^{KO}Trap1^{WT}$ mice, and decreased in $Apoe^{KO}Trap1^{SMCKO}$ mice, without any alteration in H4K8la or H4K5la. We also examined the differentiation state and phenotype of SMCs in $Apoe^{KO}Trap1^{WT}$ mice fed with an NC or HFD. We observed that in comparison with NC-fed $Apoe^{KO}Trap1^{WT}$ mice, contractile phenotype-related genes significantly decreased in HFD-fed $Apoe^{KO}Trap1^{WT}$ mice, whereas synthetic phenotype-related genes showed the opposite trend. Moreover, these changes were reversed in HFD-fed $Apoe^{KO}Trap1^{SMCKO}$ mice (see Supplementary data online, *Figure S6C and D*). These findings suggested that SMC-specific *Trap1* knockout could inhibit HFD-induced VSMC phenotype transformation. To further confirm the role of TRAP1 in mitochondria *in vivo*, seahorse data showed increased OCR levels and decreased ECAR levels in MOVAS from HFD-fed $Apoe^{KO}Trap1^{SMCKO}$ mice compared with those of $Apoe^{KO}Trap1^{WT}$ mice (*Figure 6H and I*). Lactate production and SASP expression were also significantly decreased in HFD-fed $Apoe^{KO}Trap1^{SMCKO}$ MOVAS (*Figure 6J and K*). Collectively, these results suggested that TRAP1 promotes atherosclerosis by increasing VSMC senescence via increased H4K12la levels.

Pharmacological inhibition of TRAP1 suppresses atherosclerosis development *in vivo*

To further identify the role of TRAP1 in the development of atherosclerosis, the TRAP1 inhibitor G-TPP was administered to HFD-fed

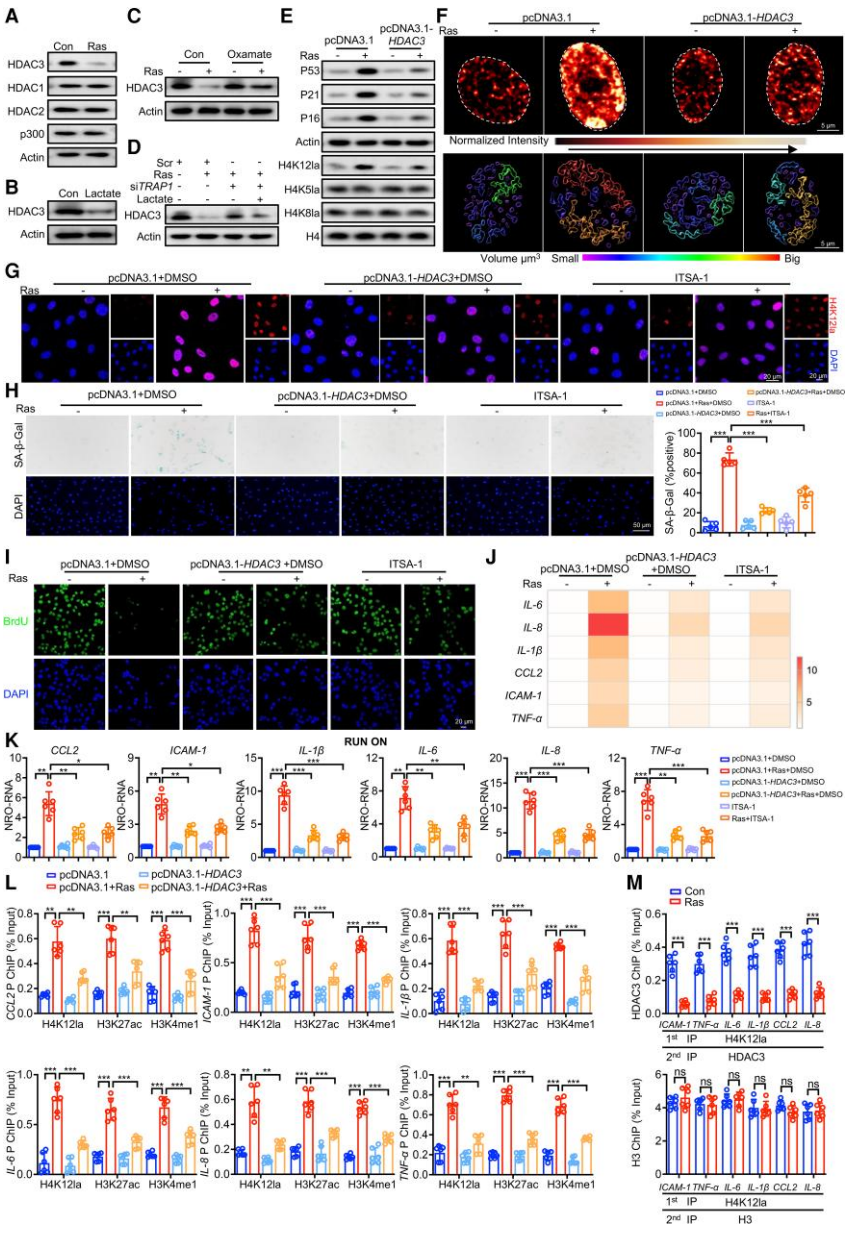

Figure 5 Up-regulation of H4K12la by blocking HDAC3 promotes senescence in VSMCs. (*A*) Western blot analysis of p300 and HDAC1–3 levels in Ras-induced hVSMCs ($n = 5$ independent biological replicates). (*B*) Western blot analysis of HDAC3 levels in hVSMCs treated with lactate ($n = 5$ independent biological replicates). (*C*) Western blot analysis of HDAC3 levels in Ras-induced hVSMCs. Ras-induced hVSMCs were treated with si*TRAP1*, followed by treatment with or without 1 mM oxamate ($n = 5$ independent biological replicates). (*D*) Western blot analysis of HDAC3 levels in Ras-induced hVSMCs following TRAP1 deficiency with or without lactate treatment ($n = 5$ independent biological replicates). (*E*) Western blot analysis of lactylation modification and senescence markers in HDAC3-overexpressing senescent hVSMCs ($n = 5$ independent biological replicates). (*F*) Expression levels of nuclear H4K12la in Ras-induced hVSMCs following HDAC3 overexpression, assessed using super-resolution fluorescence imaging (upper). Volume information of H4K12la hotspots identified in the nucleus of HDAC3-overexpressing senescent hVSMCs (bottom) (scale bar = 5 μm, $n = 5$ independent biological replicates). (*G*) Representative images of H4K12la (red) co-stained with DAPI (blue) in Ras-induced hVSMCs. Ras-induced hVSMCs were treated with HDAC3 overexpression or ITSA-1 (150 μM) for 24 h (scale bar = 20 μm, $n = 5$ independent biological replicates). (*H*) Representative SA-β-Gal staining images of Ras-induced hVSMCs with HDAC3 overexpression or ITSA-1 treatment, with quantification of SA-β-Gal-positive cells (right panel, scale bar = 50 μm, $n = 5$ independent biological replicates). (*I*) Proliferation measured using the BrdU assay in Ras-induced hVSMCs following HDAC3 overexpression or ITSA-1 treatment (scale bar = 20 μm, $n = 5$ independent biological replicates). (*J*) RT–qPCR analysis of SASP in Ras-induced hVSMCs after HDAC3 overexpression or ITSA-1 treatment, presented as a heatmap ($n = 6$ independent biological replicates). (*K*) Transcriptional regulation of SASP in Ras-induced hVSMCs following HDAC3 overexpression or ITSA-1 treatment was analysed using the run-on assay ($n = 6$ independent biological replicates). (*L*) ChIP detection of the binding sites of H4K12la, H3K27ac, and H3K4me1 at the SASP promoter region ($n = 6$ independent biological replicates). (*M*) Re-ChIP was performed in Ras-induced hVSMCs with H4K12la antibody in the first round and a pull-down with HDAC3 antibody in the second round ($n = 6$ independent biological replicates). $^{*}P < .05$, $^{**}P < .01$, $^{***}P < .001$. Data are presented as the mean ± SD. Unpaired *t*-test was used for comparison in (M). One-way ANOVA was performed in (H, K, and L)

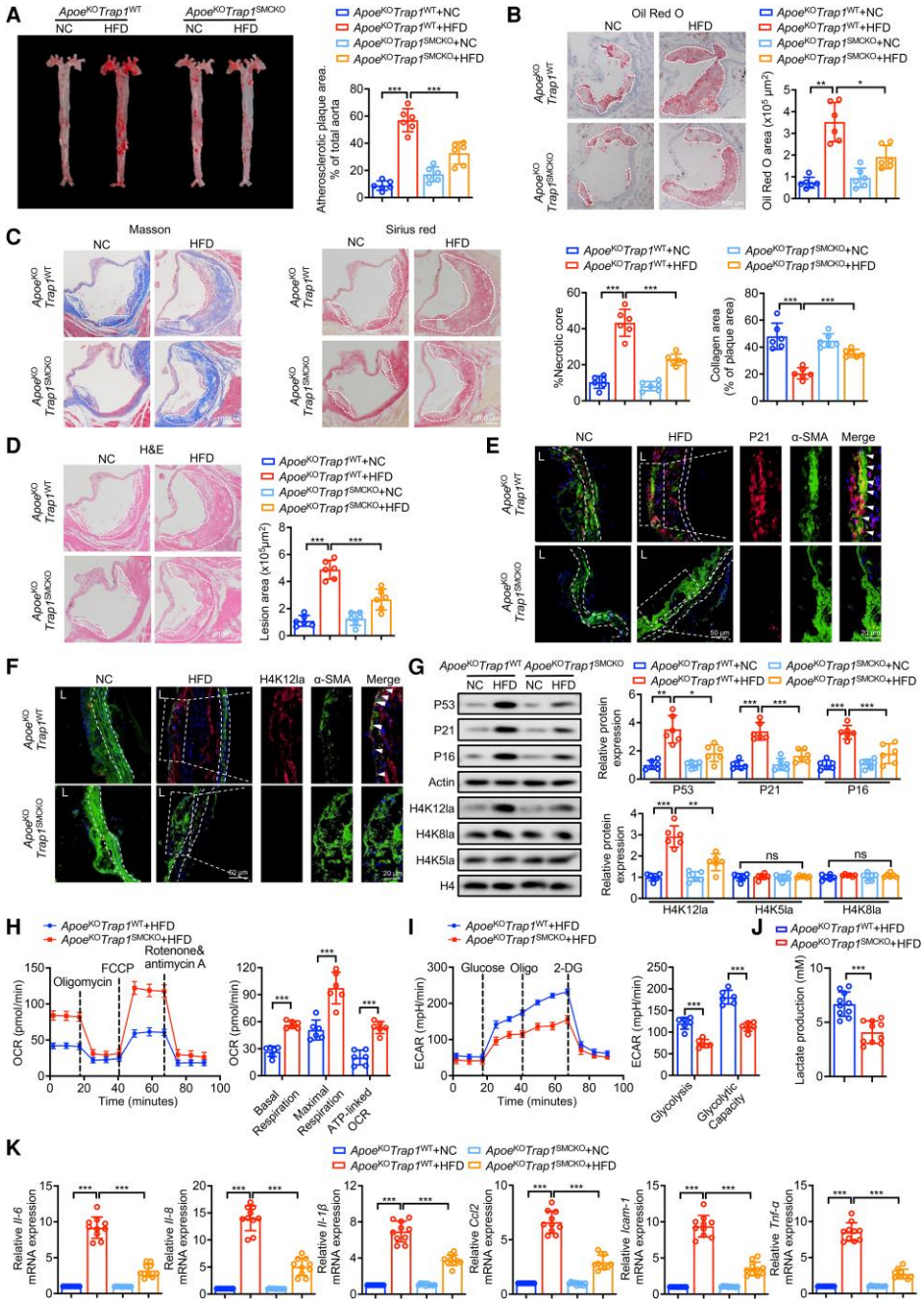

Figure 6 SMC-specific *Trap1* knockout ameliorates atherosclerosis. (*A*) Representative images of aortas stained with Oil Red O from *Apoe*^{KO}*Trap1*^{SMCKO} and *Apoe*^{KO}*Trap1*^{WT} mice fed with an NC or HFD ($n = 6$ independent biological replicates). Mice were fed with an NC or HFD for 16 weeks, from 8 weeks old. (*B–D*) Oil Red O (*B*), Masson and Sirius red (*C*), and haematoxylin and eosin (H&E) (*D*) staining of aortic roots (scale bar = 100 μm, $n = 6$ independent biological replicates). (*E*) Representative immunofluorescence staining of the SMC (α-SMA, green) and senescence (P21, red) in aortas from *Apoe*^{KO}*Trap1*^{SMCKO} and *Apoe*^{KO}*Trap1*^{WT} mice fed with an NC or HFD (scale bar = 50 μm, $n = 6$ independent biological replicates). (*F*) Representative immunofluorescence staining of the α-SMA (green) and H4K12la (red) in aortas from *Apoe*^{KO}*Trap1*^{SMCKO} and *Apoe*^{KO}*Trap1*^{WT} mice fed with an NC or HFD (scale bar = 50 μm, $n = 6$ independent biological replicates). (*G*) Western blot analysis of the expression levels of P53, P21, P16, H4K12la, H4K8la, and H4K5la in MOVAS isolated from *Apoe*^{KO}*Trap1*^{SMCKO} and *Apoe*^{KO}*Trap1*^{WT} mice fed with an NC or HFD ($n = 6$ independent biological replicates). (*H* and *I*) Seahorse analysis of the OCR (*H*) and ECAR (*I*) of MOVAS isolated from HFD-fed *Apoe*^{KO}*Trap1*^{SMCKO} and *Apoe*^{KO}*Trap1*^{WT} mice ($n = 6$ independent biological replicates). (*J*) Lactate levels in MOVAS isolated from HFD-fed *Apoe*^{KO}*Trap1*^{SMCKO} and *Apoe*^{KO}*Trap1*^{WT} mice ($n = 10$ independent biological replicates). (*K*) RT–qPCR analysis of SASP expression levels in MOVAS isolated from *Apoe*^{KO}*Trap1*^{SMCKO} and *Apoe*^{KO}*Trap1*^{WT} mice fed with an NC or HFD ($n = 10$ independent biological replicates). $^{*}P < .05$, $^{**}P < .01$, $^{***}P < .001$. Data are presented as the mean ± SD. Unpaired *t*-test was used for comparison in (*H–J*). One-way ANOVA was performed in (A–D, G, and K)

Apoe^{KO} mice. Notably, the administration of G-TPP did not affect metabolic parameters in HFD-fed *Apoe*^{KO} mice (*Figure 7A*; Supplementary data online, *Table S3*). However, G-TPP treatment markedly reduced the plaque area and necrotic core in the aortic roots of HFD-fed *Apoe*^{KO} mice while enhancing collagen content (*Figure 7B and C*). These findings suggested that G-TPP attenuates the progression of atherosclerosis. Furthermore, both P21 and H4K12la signal levels and their co-localization with α-SMA significantly decreased in HFD-fed *Apoe*^{KO} mice following G-TPP treatment, as evidenced by immunofluorescent staining (*Figure 7D*). Moreover, western blot and RT–qPCR revealed that senescence markers, H4K12la, and SASP in MOVAS were significantly reduced by G-TPP treatment (*Figure 7E and F*). Collectively, TRAP1 inhibition in VSMCs may be an effective therapeutic strategy for atherosclerosis.

Degradation of TRAP1 via PROTAC as a novel strategy for atherosclerosis treatment

Targeted protein degradation offers substantial therapeutic advantages over traditional small-molecule inhibitors, with improved efficacy, action duration, and target specificity.[39] In this context, we identified candidate compound 16b (BP3), a small molecule capable of inducing ubiquitination and subsequent degradation of TRAP1 in a cereblon (CRBN)-dependent manner (see Supplementary data online, *Figure S7A*). The initial toxicity assessment of BP3 revealed limited cell toxicity even at elevated concentrations (see Supplementary data online, *Figure S7B*). To comprehensively evaluate the properties of BP3-mediated TRAP1 degradation, we analysed TRAP1 expression in BP3-treated hVSMCs and discovered that at a concentration of 0.5 μM, BP3 induced marked degradation of TRAP1 after 6 h (*Figure 8A and B*). Moreover, BP3-induced TRAP1 degradation was counteracted by treatment with the proteasome inhibitor MG132 (*Figure 8C*). To validate the therapeutic effects of BP3 *in vivo*, HFD-fed *Apoe*^{KO} mice were administered BP3. The body weight, blood pressure, and blood lipids (cholesterol and triglycerides) did not significantly differ in mice with or without BP3 treatment (*Figure 8D*; Supplementary data online, *Table S4*). As shown in *Figure 8E*, the plaque area in the whole aorta was significantly reduced in HFD-fed *Apoe*^{KO} mice treated with BP3 compared with that in the HFD group. BP3 treatment significantly reduced the area of the aortic root plaque and the size of the necrotic core while increasing collagen content (*Figure 8F*). Furthermore, the expression of senescence makers, H4K12la, and SASP in MOVAS from HFD-fed *Apoe*^{KO} mice was consistently reduced by BP3 treatment, mirroring the effects of TRAP1 knockout (*Figure 8G and H*). Collectively, these results demonstrated that the degradation of TRAP1 using BP3 is an effective strategy for the treatment of atherosclerosis.

TRAP1 and H4K12la may be key factors involved in clinical SMC senescence and atherosclerosis

Finally, we evaluated H4K12la expression in patients with atherosclerosis and found that levels of H4K12la were markedly elevated in atherosclerotic samples (*Figure 9A*; Supplementary data online, *Table S5*). However, other common H4 lactylation sites did not change, including H4K5la and H4K8la. In addition, the expression level of H4K12la protein was positively correlated with the expression of senescence markers in atherosclerosis (*Figure 9B*). Linear regression analysis revealed a close association between changes in the mRNA levels of the senescence markers and SASP with those of *TRAP1* (*Figure 9C*). These results provide compelling evidence that TRAP1 and H4K12la play integral roles in the regulation of cellular senescence and human atherosclerosis.

Discussion

In our study, we observed that the physiological role of mitochondrial protein TRAP1 undergoes dramatic changes, inducing alterations in the histone microenvironment and promoting VSMC senescence and atherosclerosis. Mechanistically, TRAP1 up-regulated glycolysis, leading to increased lactate accumulation. Subsequently, this elevated lactate level enhanced H4K12la via the histone lysine delactylase, HDAC3. Moreover, H4K12la was significantly enriched at the SASP promoter, thereby facilitating nascent SASP transcription and exacerbating atherosclerosis (*Structured Graphical Abstract*). This study revealed a novel cross-talk between cellular metabolism and epigenetic modulation during cellular senescence, highlighting TRAP1 as a potential therapeutic target in atherosclerosis.

Cellular senescence, characterized by stress-induced cell cycle arrest, is linked to various diseases, including cardiovascular diseases and non-alcoholic steatohepatitis.[40] Disruption of energy metabolism and mitochondrial dysfunction substantially contribute to cellular senescence.[41] Mitochondrial damage poses challenges for ATP production via mitochondrial oxidative phosphorylation, forcing a shift to glycolysis, an emerging hallmark of metabolic dysfunction.[42] Our findings indicated an increase in glycolysis in senescent VSMCs, prompting further exploration of potential mechanisms underlying metabolic reprogramming in these cells.

TRAP1 is a crucial regulator of mitochondrial bioenergetics and plays a pivotal role in maintaining mitochondrial homeostasis.[43] *Trap1* knockout mice exhibit a reduced incidence of age-related illnesses.[44] Despite its established role in mitochondrial function and ageing-related diseases, the involvement of TRAP1 in VSMC senescence has not been explored before. In this study, we found that TRAP1 was overexpressed in senescent VSMCs, contributing to the up-regulation of glycolysis and down-regulation of the TCA metabolic pathway.

Consistently, TRAP1 promotes glycolysis in senescent VSMCs by preventing the ubiquitination of the glycolytic rate-limiting enzyme PFK1 via protein–protein interaction.[18] Cellular senescence is recognized as a mechanism that prevents cancer.[45] Accumulating evidence suggests that senescent cells accumulate with age, creating a tissue microenvironment that promotes cancer.[46,47] Therefore, exploring the use of oncology drugs to treat senescence-driven cardiovascular diseases is warranted. Tamoxifen, a breast cancer treatment drug, reduces oxidative damage associated with atherosclerosis.[48] Notably, our findings indicated that the TRAP1 inhibitor G-TPP, a clinical phase I antitumour agent, effectively reduced plaque formation, suggesting its potential as a drug for treating atherosclerosis. This highlights the potential for repurposing oncological drugs to address senescence-related cardiovascular conditions, providing a novel avenue for therapeutic exploration.

The PROTAC BP3 is a heterobifunctional molecule that triggers TRAP1 ubiquitin degradation by inducing TRAP1 proximity to the E3 ligase.[49] PROTAC offers numerous advantages over conventional small molecule inhibitors, including high selectivity and low toxicity.[50] Therefore, developing innovative PROTAC systems to treat atherosclerosis is imperative. We found that BP3 effectively induced TRAP1

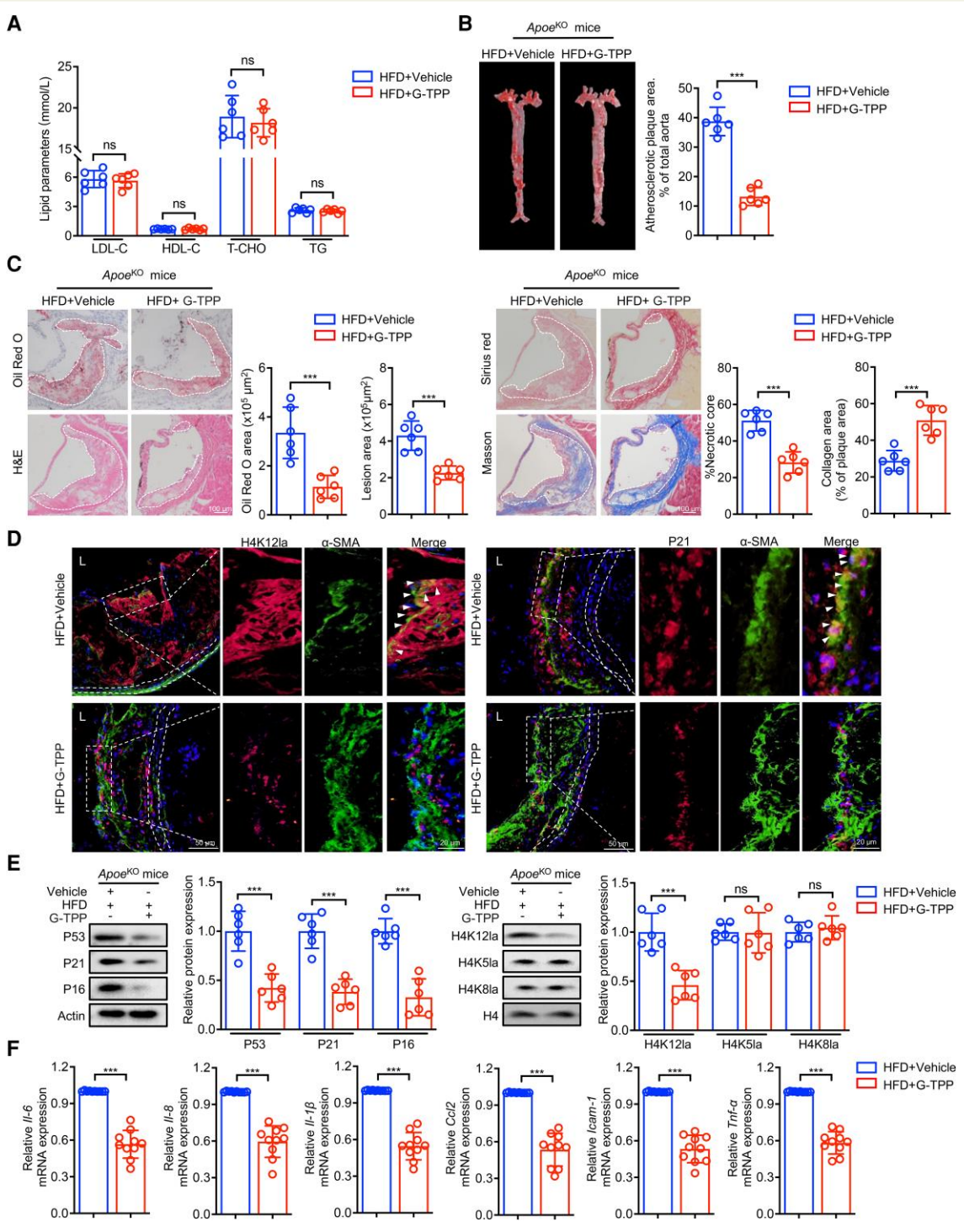

Figure 7 Pharmacological inhibition of TRAP1 suppresses atherosclerosis development *in vivo*. (*A*) The HFD-fed *Apoe*^{KO} mice were intraperitoneally administered with G-TPP or vehicle (Vehicle control) for 12 weeks. The plasma levels of LDL-cholesterol (LDL-C), HDL-cholesterol (HDL-C), total cholesterol (T-CHO), and triglyceride (TG) in mice were measured ($n = 6$ independent biological replicates). (*B*) En face aortas stained with Oil Red O from HFD-fed *Apoe*^{KO} mice with or without G-TPP treatment ($n = 6$ independent biological replicates). (*C*) The Oil Red O, H&E, Masson, and Sirius red staining of aortic roots from HFD-fed *Apoe*^{KO} mice with or without G-TPP treatment (scale bar = 100 μm, $n = 6$ independent biological replicates). (*D*) Representative immunostaining images of H4K12la (red) and P21 (red) in aortas from HFD-fed *Apoe*^{KO} mice with or without G-TPP treatment (scale bar = 50 μm, $n = 6$ independent biological replicates). (*E*) Protein levels of P53, P21, P16, H4K12la, H4K5la, and H4K8la in MOVAS from HFD-fed *Apoe*^{KO} mice with or without G-TPP treatment were measured by western blot ($n = 6$ independent biological replicates). (*F*) The expression levels of SASP in MOVAS from HFD-fed *Apoe*^{KO} mice with or without G-TPP treatment were examined using RT–qPCR ($n = 10$ independent biological replicates). *$P < .05$, **$P < .01$, ***$P < .001$. Data are presented as the mean ± SD. Unpaired *t*-test was used for comparison in (A–C, E, and F)

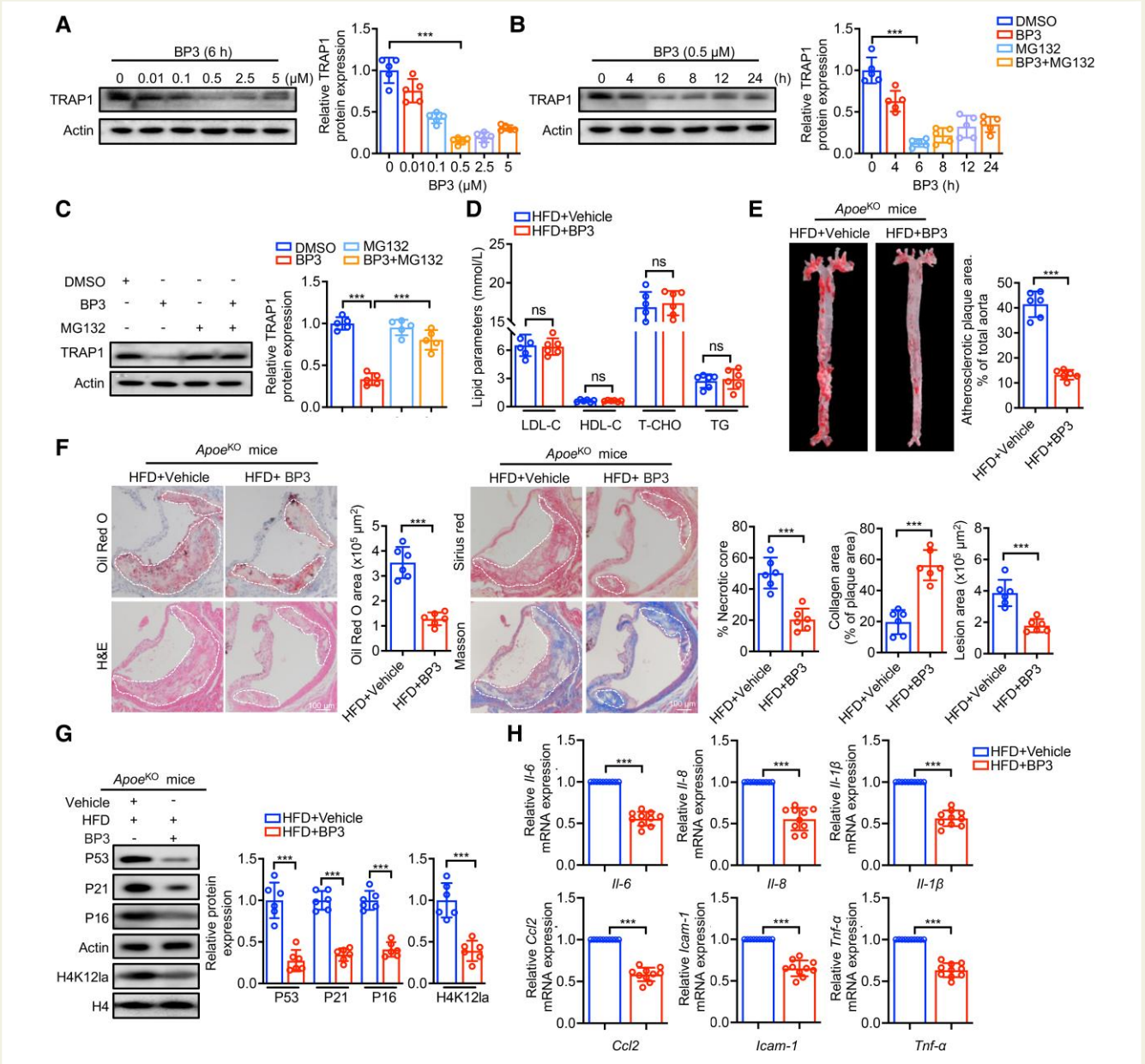

Figure 8 Degradation of TRAP1 via PROTAC as a novel strategy for atherosclerosis treatment. (*A*) Western blot analysis of the expression of TRAP1 in hVSMCs. hVSMCs were treated with BP3 (6 h) at different concentrations ($n = 5$ independent biological replicates). (*B*) Western blot analysis of TRAP1 expression in hVSMCs. hVSMCs were treated with BP3 (0.5 μM) at different time points ($n = 5$ independent biological replicates). (*C*) Western blot analysis of TRAP1 expression in hVSMCs. hVSMCs were treated with BP3 (0.5 μM) for 6 h, followed by treatment with or without 20 μM MG132 for 6 h ($n = 5$ independent biological replicates). (*D*) Plasma levels of LDL-C, HDL-C, T-CHO, and TG in HFD-fed *Apoe*^{KO} mice. Mice were intraperitoneally administered with BP3 or vehicle (Vehicle control) for 12 weeks ($n = 6$ independent biological replicates). (*E*) En face aortas, stained with Oil Red O, from HFD-fed *Apoe*^{KO} mice with or without BP3 treatment (left panel). Quantification of the plaque area as a percentage of the total aortic area (right panel, $n = 6$ independent biological replicates). (*F*) The Oil Red O, H&E, Masson, and Sirius red staining of aortic roots from HFD-fed *Apoe*^{KO} mice with or without BP3 treatment (scale bar = 100 μm, $n = 6$ independent biological replicates). (*G*) Protein levels of P53, P21, P16, and H4K12la in MOVAS from HFD-fed *Apoe*^{KO} mice with or without BP3 treatment, measured using western blot analysis ($n = 6$ independent biological replicates). (*H*) The expression levels of SASP in MOVAS from HFD-fed *Apoe*^{KO} mice with or without BP3 treatment, examined via RT–qPCR ($n = 10$ independent biological replicates). *$P < .05$, **$P < .01$, ***$P < .001$. Data are presented as the mean ± SD. Unpaired *t*-test was used for comparison in (D–H). One-way ANOVA was performed in (A–C)

protein degradation and significantly reduced VSMC senescence and atherosclerosis *in vitro* and *in vivo*. Therefore, BP3 is a promising drug candidate for the treatment of atherosclerosis.

Histone lactylation, as a newly identified epigenetic modification, plays a considerable role in various biological processes. It is enriched at the promoters of glycolytic genes and exacerbates microglial

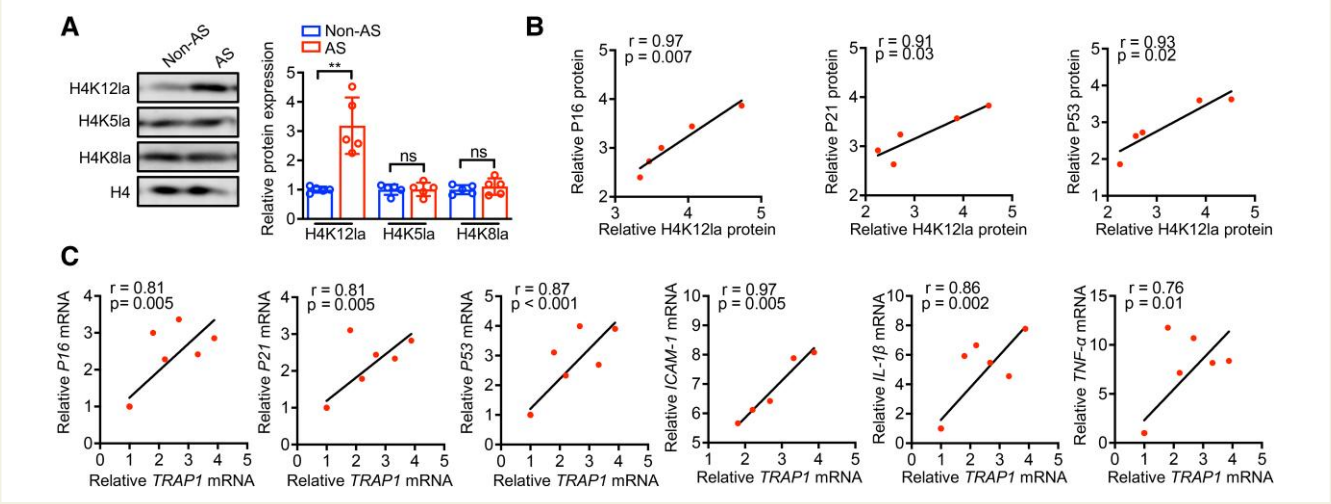

Figure 9 TRAP1 and H4K12la may be key factors involved in clinical SMC senescence and atherosclerosis. (*A*) Western blot analysis of H4K12la, H4K5la, and H4K8la in patients with atherosclerosis and healthy individuals ($n = 5$ independent biological replicates). (*B*) Linear regression analysis of H4K12la protein expression with P53, P21, and P16 protein expression in aortic tissues from patients with atherosclerosis. (*C*) Linear regression analysis of TRAP1 mRNA with senescence markers and SASP in aortic tissues from patients with atherosclerosis. $^{*}P < .05$, $^{**}P < .01$, $^{***}P < .001$. Data are presented as the mean ± SD. Unpaired *t*-test was used for comparison in (A). Correlation analysis was performed in (B and C)

dysfunction in Alzheimer's disease by increasing glycolytic activity.[24] These findings highlight the importance of histone lactylation in cellular functions and its potential implications in disease processes. Our research showed that H4K12la, a distinctive histone lactylation modification, promotes the activation of the SASP, which is associated with senescence. Moreover, a strong association between H4K12la and the expression of H3K27ac and H3K4me3 exists, together creating a senescence-specific chromatin microenvironment.

Various enzymes involved in histone lactylation include p300 and the HDAC1–3 family. In macrophages, p300 is an essential writer of histone lactylation.[37,51] However, our study revealed that HDAC3, a member of the HDAC family known for its histone deacetylation activity, was the most relevant enzyme for histone lactylation during VSMC senescence.[52] HDAC3 promotes DNA damage repair and represses tumour-associated gene transcription by converting H9K3ac (acetylated histone H3 lysine 9) to H9K3me3 (trimethylated histone H3 lysine 9).[53] However, HDAC3 expression was inhibited, leading to increased levels of H4K12la, enhanced SASP expression, and promotion of VSMC senescence. These findings provide novel targets for the treatment of atherosclerosis.

Recent studies have highlighted the importance of mitonuclear communication in maintaining cellular homeostasis.[8] Cellular energy metabolism provides specific substrates or cofactors for histone modifications, regulating gene transcription and contributing to disease progression.[54] Lactate, a by-product of aerobic glycolysis, has been implicated in histone lactylation and participates in various pathological processes. Histone lactylation promotes early activation of the reparative transcriptional response in monocytes, which is crucial for establishing immune homeostasis and initiating cardiac repair after myocardial infarction.[55] Additionally, H4K12la exacerbates microglial dysfunction in Alzheimer's disease by regulating PKM2.[24] Notably, our study revealed emerging links between lactate metabolism and epigenetics. Chromatin serves as the signal integration and storage platform, attracting the metabolic signalling molecule lactate, forming the TRAP1–lactate–histone lactylation axis in senescent hVSMCs and atherosclerosis. This perspective of metabolic–epigenetic cross-talk supplements classical ageing-related signalling pathways. Further investigation of potential cross-talk between other metabolic intermediates and emerging histone modifications holds promise for discovering previously unknown mechanisms underlying cellular senescence, atherosclerosis, and other diseases.

It is important to acknowledge the limitations of this study. We observed that the up-regulation of lactate in senescent SMCs substantially and selectively inhibited HDAC3 expression. Although HDAC1 and HDAC3 are the most effective lysine lactylation modification 'erasers', and lactate is recognized as a non-selective HDAC inhibitor,[37,56] the precise mechanism by which lactate identifies and regulates HDAC3 in senescent SMCs remains unclear, and requires further investigation.

In summary, we demonstrated that HDAC3, a unique histone lysine delactylase, is a pivotal regulator of H4K12la in senescent VSMCs, promoting SASP expression and contributing to VSMC senescence. This study provides valuable insights into the connection between energy metabolism reprogramming and epigenetic modifications, revealing a novel mechanism underlying cellular senescence. Furthermore, our findings highlight the importance of TRAP1 in facilitating mitonuclear communication and suggest that TRAP1 inhibition could be a promising therapeutic strategy for atherosclerosis.

Supplementary Data

Supplementary data are available at *European Heart Journal* online.

Declarations

Disclosure of Interest

All authors declare no disclosure of interest for this contribution.

Data Availability

The data on which this article is based will be shared at the reasonable request of the corresponding author.

Funding

This work was supported by the National Natural Science Foundation of China (grant nos 82270421, 81970428, 31771334, 81800385, 82270484, 82121001, 82030013, 82241211, 91639303, and 81770441), the National Key Research and Development Program of China (2019YFA0802704), and the British Heart Foundation (PG/22/11217).

Ethical Approval

All animal experimental protocols were approved by the Animal Ethics Committee of Nanjing Medical University. All experimental protocols using human aortic samples were approved by the Affiliated Drum Tower Hospital of Nanjing University Medical School (2019-219-01).

Pre-registered Clinical Trial Number

Not applicable.

References

1. Bennett MR, Sinha S, Owens GK. Vascular smooth muscle cells in atherosclerosis. *Circ Res* 2016;**118**:692–702. https://doi.org/10.1161/CIRCRESAHA.115.306361
2. Bi X, Du C, Wang X, Wang X-Y, Han W, Wang Y, *et al.* Mitochondrial damage-induced innate immune activation in vascular smooth muscle cells promotes chronic kidney disease-associated plaque vulnerability. *Adv Sci (Weinh)* 2021;**8**:2002738. https://doi.org/10.1002/advs.202002738
3. Grootaert MOJ, Moulis M, Roth L, Martinet W, Vindis C, Bennett MR, *et al.* Vascular smooth muscle cell death, autophagy and senescence in atherosclerosis. *Cardiovasc Res* 2018;**114**:622–34. https://doi.org/10.1093/cvr/cvy007
4. Collado M, Blasco MA, Serrano M. Cellular senescence in cancer and aging. *Cell* 2007;**130**:223–33. https://doi.org/10.1016/j.cell.2007.07.003
5. Wang K, Liu H, Hu Q, Wang L, Liu J, Zheng Z, *et al.* Epigenetic regulation of aging: implications for interventions of aging and diseases. *Signal Transduct Target Ther* 2022;**7**:374. https://doi.org/10.1038/s41392-022-01211-8
6. Behmoaras J, Gil J. Similarities and interplay between senescent cells and macrophages. *J Cell Biol* 2021;**220**:e202010162. https://doi.org/10.1083/jcb.202010162
7. Gorenne I, Kavurma M, Scott S, Bennett M. Vascular smooth muscle cell senescence in atherosclerosis. *Cardiovasc Res* 2006;**72**:9–17. https://doi.org/10.1016/j.cardiores.2006.06.004
8. Zhu D, Li X, Tian Y. Mitochondrial-to-nuclear communication in aging: an epigenetic perspective. *Trends Biochem Sci* 2022;**47**:645–59. https://doi.org/10.1016/j.tibs.2022.03.008
9. Shi L, Tu BP. Acetyl-CoA and the regulation of metabolism: mechanisms and consequences. *Curr Opin Cell Biol* 2015;**33**:125–31. https://doi.org/10.1016/j.ceb.2015.02.003
10. Oller J, Gabandé-Rodríguez E, Ruiz-Rodríguez MJ, Desdín-Micó G, Aranda JF, Rodrigues-Diez R, *et al.* Extracellular tuning of mitochondrial respiration leads to aortic aneurysm. *Circulation* 2021;**143**:2091–109. https://doi.org/10.1161/circulationaha.120.051171
11. Li X, Yang Y, Zhang B, Lin X, Fu X, An Y, *et al.* Lactate metabolism in human health and disease. *Signal Transduct Target Ther* 2022;**7**:305. https://doi.org/10.1038/s41392-022-01151-3
12. Cluntun AA, Badolia R, Lettlova S, Parnell KM, Shankar TS, Diakos NA, *et al.* The pyruvate–lactate axis modulates cardiac hypertrophy and heart failure. *Cell Metab* 2021;**33**:629–648.e10. https://doi.org/10.1016/j.cmet.2020.12.003
13. Dabral S, Muecke C, Valasarajan C, Schmoranzer M, Wietelmann A, Semenza GL, *et al.* A RASSF1A–HIF1α loop drives Warburg effect in cancer and pulmonary hypertension. *Nat Commun* 2019;**10**:2130. https://doi.org/10.1038/s41467-019-10044-z
14. Hirschhaeuser F, Sattler UG, Mueller-Klieser W. Lactate: a metabolic key player in cancer. *Cancer Res* 2011;**71**:6921–5. https://doi.org/10.1158/0008-5472.Can-11-1457
15. Ross JM, Oberg J, Brene S, Coppotelli G, Terzioglu M, Pernold K, *et al.* High brain lactate is a hallmark of aging and caused by a shift in the lactate dehydrogenase A/B ratio. *Proc Natl Acad Sci USA* 2010;**107**:20087–92. https://doi.org/10.1073/pnas.1008189107
16. Fitzgerald JC, Zimprich A, Carvajal Berrio DA, Schindler KM, Maurer B, Schulte C, *et al.* Metformin reverses TRAP1 mutation-associated alterations in mitochondrial function in Parkinson's disease. *Brain* 2017;**140**:2444–59. https://doi.org/10.1093/brain/awx202
17. Serapian SA, Sanchez-Martín C, Moroni E, Rasola A, Colombo G. Targeting the mitochondrial chaperone TRAP1: strategies and therapeutic perspectives. *Trends Pharmacol Sci* 2021;**42**:566–76. https://doi.org/10.1016/j.tips.2021.04.003
18. Maddalena F, Condelli V, Matassa DS, Pacelli C, Scrima R, Lettini G, *et al.* TRAP1 enhances Warburg metabolism through modulation of PFK1 expression/activity and favors resistance to EGFR inhibitors in human colorectal carcinomas. *Mol Oncol* 2020;**14**:3030–47. https://doi.org/10.1002/1878-0261.12814
19. Ramos Rego I, Silverio D, Eufrasio MI, Pinhancos SS, Lopes da Costa B, Teixeira J, *et al.* TRAP1 is expressed in human retinal pigment epithelial cells and is required to maintain their energetic status. *Antioxidants (Basel)* 2023;**12**:381. https://doi.org/10.3390/antiox12020381
20. Costa AC, Loh SHY, Martins LM. Drosophila trap1 protects against mitochondrial dysfunction in a PINK1/parkin model of Parkinson's disease. *Cell Death Dis* 2013;**4**:e467. https://doi.org/10.1038/cddis.2012.205
21. Xie S, Xu S-C, Deng W, Tang Q. Metabolic landscape in cardiac aging: insights into molecular biology and therapeutic implications. *Signal Transduct Target Ther* 2023;**8**:114. https://doi.org/10.1038/s41392-023-01378-8
22. Cruz C, Della Rosa M, Krueger C, Gao Q, Horkai D, King M, *et al.* Tri-methylation of histone H3 lysine 4 facilitates gene expression in ageing cells. *Elife* 2018;**7**:e34081. https://doi.org/10.7554/eLife.34081
23. Zhang D, Tang Z, Huang H, Zhou G, Cui C, Weng Y, *et al.* Metabolic regulation of gene expression by histone lactylation. *Nature* 2019;**574**:575–80. https://doi.org/10.1038/s41586-019-1678-1
24. Pan RY, He L, Zhang J, Liu X, Liao Y, Gao J, *et al.* Positive feedback regulation of microglial glucose metabolism by histone H4 lysine 12 lactylation in Alzheimer's disease. *Cell Metab* 2022;**34**:634–48. https://doi.org/10.1016/j.cmet.2022.02.013
25. Jellinghaus S. Genexpressionsanalyse von humaner koronarer atherosklerotischer plaque. PhD thesis, Deutsches Herzzentrum München, 2006.
26. Sun N, Youle RJ, Finkel T. The mitochondrial basis of aging. *Mol Cell* 2016;**61**:654–66. https://doi.org/10.1016/j.molcel.2016.01.028
27. Shen W, Song Z, Zhong X, Huang M, Shen D, Gao P, *et al.* Sangerbox: a comprehensive, interaction-friendly clinical bioinformatics analysis platform. *iMeta* 2022;**1**:e36. https://doi.org/10.1002/imt2.36
28. Gorgoulis V, Adams PD, Alimonti A, Bennett DC, Bischof O, Bishop C, *et al.* Cellular senescence: defining a path forward. *Cell* 2019;**179**:813–27. https://doi.org/10.1016/j.cell.2019.10.005
29. Cao G, Xuan X, Hu J, Zhang R, Jin H, Dong H. How vascular smooth muscle cell phenotype switching contributes to vascular disease. *Cell Commun Signal* 2022;**20**:180. https://doi.org/10.1186/s12964-022-00993-2
30. Wiley CD, Campisi J. The metabolic roots of senescence: mechanisms and opportunities for intervention. *Nat Metab* 2021;**3**:1290–301. https://doi.org/10.1038/s42255-021-00483-8
31. Cannino G, Urbani A, Gaspari M, Varano M, Negro A, Filippi A, *et al.* The mitochondrial chaperone TRAP1 regulates F-ATP synthase channel formation. *Cell Death Differ* 2022;**29**:2335–46. https://doi.org/10.1038/s41418-022-01020-0
32. Li W, Xu Z, Hong J, Xu Y. Expression patterns of three regulation enzymes in glycolysis in esophageal squamous cell carcinoma: association with survival. *Med Oncol* 2014;**31**:118. https://doi.org/10.1007/s12032-014-0118-1
33. Diaz-Ruiz R, Averet N, Araiza D, Pinson B, Uribe-Carvajal S, Devin A, *et al.* Mitochondrial oxidative phosphorylation is regulated by fructose 1,6-bisphosphate. A possible role in Crabtree effect induction? *J Biol Chem* 2008;**283**:26948–55. https://doi.org/10.1074/jbc.M800408200
34. Shannon P, Markiel A, Ozier O, Baliga NS, Wang JT, Ramage D, *et al.* Cytoscape: a software environment for integrated models of biomolecular interaction networks. *Genome Res* 2003;**13**:2498–504. https://doi.org/10.1101/gr.1239303
35. Sun X, He L, Liu H, Thorne RF, Zeng T, Liu L, *et al.* The diapause-like colorectal cancer cells induced by SMC4 attenuation are characterized by low proliferation and chemotherapy insensitivity. *Cell Metab* 2023;**35**:1563–79. https://doi.org/10.1016/j.cmet.2023.07.005
36. Yashar WM, Kong G, VanCampen J, Curtiss BM, Coleman DJ, Carbone L, *et al.* Gopeaks: histone modification peak calling for CUT&Tag. *Genome Biol* 2022;**23**:144. https://doi.org/10.1186/s13059-022-02707-w
37. Moreno-Yruela C, Zhang D, Wei W, Baek M, Liu W, Gao J, *et al.* Class I histone deacetylases (HDAC1–3) are histone lysine delactylases. *Sci Adv* 2022;**8**:eabi6696. https://doi.org/10.1126/sciadv.abi6696
38. Latham T, Mackay L, Sproul D, Karim M, Culley J, Harrison DJ, *et al.* Lactate, a product of glycolytic metabolism, inhibits histone deacetylase activity and promotes changes in gene expression. *Nucleic Acids Res* 2012;**40**:4794–803. https://doi.org/10.1093/nar/gks066
39. Si J, Shi X, Sun S, Zou B, Li Y, An D, *et al.* Hematopoietic progenitor kinase1 (HPK1) mediates T cell dysfunction and is a druggable target for T cell-based immunotherapies. *Cancer Cell* 2020;**38**:551–66. https://doi.org/10.1016/j.ccell.2020.08.001
40. Evangelou K, Vasileiou PVS, Papaspyropoulos A, Hazapis O, Petty R, Demaria M, *et al.* Cellular senescence and cardiovascular diseases: moving to the 'heart' of the problem. *Physiol Rev* 2023;**103**:609–47. https://doi.org/10.1152/physrev.00007.2022
41. Coryell PR, Diekman BO, Loeser RF. Mechanisms and therapeutic implications of cellular senescence in osteoarthritis. *Nat Rev Rheumatol* 2021;**17**:47–57. https://doi.org/10.1038/s41584-020-00533-7
42. Lavie J, De Belvalet H, Sonon S, Ion AM, Dumon E, Melser S, *et al.* Ubiquitin-dependent degradation of mitochondrial proteins regulates energy metabolism. *Cell Rep* 2018;**23**:2852–63. https://doi.org/10.1016/j.celrep.2018.05.013

43. Im C-N, Seo J-S. Overexpression of tumor necrosis factor receptor-associated protein 1 (TRAP1), leads to mitochondrial aberrations in mouse fibroblast NIH/3T3 cells. *BMB Rep* 2014;**47**:280–5. https://doi.org/10.5483/bmbrep.2014.47.5.174
44. Lisanti S, Tavecchio M, Chae YC, Liu Q, Brice AK, Thakur ML, *et al.* Deletion of the mitochondrial chaperone TRAP-1 uncovers global reprogramming of metabolic networks. *Cell Rep* 2014;**8**:671–7. https://doi.org/10.1016/j.celrep.2014.06.061
45. Birch J, Gil J. Senescence and the SASP: many therapeutic avenues. *Genes Dev* 2020;**34**:1565–76. https://doi.org/10.1101/gad.343129.120
46. Campisi J. Aging, cellular senescence, and cancer. *Annu Rev Physiol* 2013;**75**:685–705. https://doi.org/10.1146/annurev-physiol-030212-183653
47. López-Otín C, Pietrocola F, Roiz-Valle D, Galluzzi L, Kroemer G. Meta-hallmarks of aging and cancer. *Cell Metab* 2023;**35**:12–35. https://doi.org/10.1016/j.cmet.2022.11.001
48. Williams JK, Wagner JD, Li Z, Golden DL, Adams MR. Tamoxifen inhibits arterial accumulation of LDL degradation products and progression of coronary artery atherosclerosis in monkeys. *Arterioscler Thromb Vasc Biol* 1997;**17**:403–8. https://doi.org/10.1161/01.atv.17.2.403
49. Liu Q, Tu G, Hu Y, Jiang Q, Liu J, Lin S, *et al.* Discovery of BP3 as an efficacious proteolysis targeting chimera (PROTAC) degrader of HSP90 for treating breast cancer. *Eur J Med Chem* 2022;**228**:114013. https://doi.org/10.1016/j.ejmech.2021.114013
50. Guenette RG, Yang SW, Min J, Pei B, Potts PR. Target and tissue selectivity of PROTAC degraders. *Chem Soc Rev* 2022;**51**:5740–56. https://doi.org/10.1039/d2cs00200k
51. Ghosh AK. P300 in cardiac development and accelerated cardiac aging. *Aging Dis* 2020;**11**:916–26. https://doi.org/10.14336/ad.2020.0401
52. Moreno-Yruela C, Bæk M, Monda F, Olsen CA. Chiral posttranslational modification to lysine ε-amino groups. *Acc Chem Res* 2022;**55**:1456–66. https://doi.org/10.1021/acs.accounts.2c00115
53. Ji H, Zhou Y, Zhuang X, Zhu Y, Wu Z, Lu Y, *et al.* HDAC3 deficiency promotes liver cancer through a defect in H3K9ac/H3K9me3 transition. *Cancer Res* 2019;**79**:3676–88. https://doi.org/10.1158/0008-5472.Can-18-3767
54. Ly CH, Lynch GS, Ryall JG. A metabolic roadmap for somatic stem cell fate. *Cell Metab* 2020;**31**:1052–67. https://doi.org/10.1016/j.cmet.2020.04.022
55. Wang N, Wang W, Wang X, Mang G, Chen J, Yan X, *et al.* Histone lactylation boosts reparative gene activation post-myocardial infarction. *Circ Res* 2022;**131**:893–908. https://doi.org/10.1161/circresaha.122.320488
56. Feng Q, Liu Z, Yu X, Huang T, Chen J, Wang J, *et al.* Lactate increases stemness of CD8+ T cells to augment anti-tumor immunity. *Nat Commun* 2022;**13**:4981. https://doi.org/10.1038/s41467-022-32521-8